Diabetologia (2006) 49:2948–2958
DOI 10.1007/s00125-006-0432-z

ARTICLE

Streptozotocin-induced partial beta cell depletion in nude mice without hyperglycaemia induces pancreatic morphogenesis in transplanted embryonic stem cells

F. Takeshita · M. Kodama · H. Yamamoto · Y. Ikarashi · S. Ueda · T. Teratani · Y. Yamamoto · T. Tamatani · S. Kanegasaki · T. Ochiya · G. Quinn

Received: 30 May 2006 / Accepted: 27 July 2006 / Published online: 18 October 2006

Abstract
Aims/hypothesis It appears that the adult pancreas has limited regenerative ability following beta cell destruction by streptozotocin (STZ). However, it is not clear if this limitation is due to an inability to respond to, rather than an absence of, regenerative stimuli. In this study we aimed to uncouple the regenerative signal from the regenerative response by using an exogenous stem cell source to detect regenerative stimuli produced by the STZ-injured pancreas at physiological blood glucose levels.
Method Adult nude mice received 150 mg/kg STZ and 1×10^6 J1 mouse embryonic stem (ES) cells by i.p. injection. Permanent beta cell depletion of 50% was estimated from the ratio of beta:alpha cells in pancreata from STZ-treated mice compared with control animals after 24 days.
Results Transplanted ES cells homed to the STZ-injured pancreas and formed tumours. Immunocytochemical analysis of pancreas-associated ES tumours revealed foci containing insulin/PDX-1 double-positive and glucagon-positive/PDX-1-negative cell clusters associated with PDX-1-positive columnar lumenal epithelium and extensive α-amylase-positive pancreatic acini comprising approximately 0.1% of ES tumour volume.
Conclusions/interpretation These data indicate that (1) the adult pancreas produces a milieu of regenerative stimuli following beta cell destruction, and (2) this is not dependent on hyperglycaemic conditions; (3) these regenerative stimuli appear to recapitulate the signalling pathways of embryonic development, since both exocrine and endocrine lineages are produced from PDX-1-positive precursor epithelium. This model will be useful for characterising the regenerative mechanisms in the adult pancreas.

Keywords α-amylase · Embryonic stem cells · Glucagon · Insulin · Morphogenesis · PDX-1 · Regeneration · Streptozotocin · Transplantation

Abbreviations

DAPI	4′,6-diamidino-2-phenylindole
E	embryonic day
ES	embryonic stem (cells)
ESM	Electronic supplementary material
IVIS	in vivo imaging system
PDX-1	pancreatic and duodenal homeobox protein-1
STZ	streptozotocin

Electronic supplementary material Supplementary material is available in the online version of this article at http://dx.doi.org/10.1007/s00125-006-0432-z and is accessible to authorised users.

F. Takeshita · M. Kodama · H. Yamamoto · S. Ueda · T. Teratani · Y. Yamamoto · T. Ochiya · G. Quinn (✉)
Section for Studies on Metastasis,
National Cancer Center Research Institute,
1-1 Tsukiji, 5-chome, Chuo-ku,
Tokyo 104-0045, Japan
e-mail: garyquinn99@hotmail.com

T. Tamatani · S. Kanegasaki · G. Quinn
Effector Cell Institute, Research Center for Advanced Science and Technology (RCAST), University of Tokyo,
Tokyo, Japan

Y. Ikarashi
Pharmacology Division,
National Cancer Center Research Institute,
Tokyo, Japan

Introduction

Current mainstream treatments for type 1 (insulin-dependent) diabetes are frequently dogged by risks of hypoglycaemic episodes, increased body weight and numerous lifestyle restrictions [1]. On the other hand, type 2 (non-

insulin-dependent) diabetes is spreading at an epidemic pace in the developing world. Hence, there is a pressing need for superior treatments, which will benefit from deciphering the mechanisms of islet beta cell regeneration. The adult pancreas has the ability to regenerate following injury by a variety of means, although this regenerative capacity appears to be limited [2–5].

Streptozotocin (STZ) is a glucose-conjugated nitrosourea taken up via the pancreas-specific GLUT2 transporter. A single high dose of STZ can induce acute hyperglycaemia by rapid necrosis of pancreatic beta cells within 24 h [3], while multiple low doses of STZ can produce a gradual onset of hyperglycaemia by T cell-mediated autoimmune destruction of beta cells, a model sharing characteristics with type 1 diabetes [6]. Early studies in the hyperglycaemic rodent indicated that following a high dose of STZ, some but not significant numbers of beta cells were recovered [7]. A lower dose of STZ, producing less severe hyperglycaemia, resulted in permanent beta cell damage with negligible replacement of beta cells from the duct [8, 9]. However, it is not clear from these studies whether the lack of beta cell recovery in STZ-treated animals with normal blood glucose levels resulted from an absence of regenerating factors or from an inability of potential endogenous beta cell progenitors to respond to nascent regenerating stimuli.

We reported that following transplantation, undifferentiated mouse embryonic stem (ES) cells migrated to the liver and formed tumours in animals with hepatic injury [10]. These ES cell tumours contained differentiated hepatocytes induced by regenerating factors from the injured liver. The aim of the present study was to investigate the lack of beta cell recovery by introducing an exogenous multi-potent cell source to the nude mouse following a single STZ dose that induced partial beta cell destruction with neither the induction of hyperglycaemia nor the knock-on effect of T cell-mediated further beta cell damage.

We investigate whether moderate STZ-induced pancreatic injury can stimulate induction of pancreas morphogenesis in transplanted ES cells as well as self-regeneration. This approach could be important for unravelling the adult pancreas regeneration process and for identifying potential soluble factors for in vitro differentiation of insulin-producing beta cells for the treatment of diabetes.

Materials and methods

Animals and STZ treatment

Animal experiments in the present study were performed in compliance with the guidelines of the Institute for Laboratory Animal Research at the National Cancer Center Research Institute (Tokyo, Japan). In addition, the Principles of Laboratory Animal Care (NIH publication no. 85-23, revised 1985; available from http://grants1.nih.gov/grants/olaw/references/phspol.htm, last accessed in July 2006) were followed. Female BALB/c nude mice (CLEA, Tokyo, Japan) aged 7 weeks were used as recipients for ES cell transplantation. Mice received a single 300-μl i.p. dose of STZ (Sigma Aldrich, St Louis, MO, USA) within 20 min of dissolution in freshly prepared 20 mmol/l cold citrate buffer (pH 4.5) at a dose ranging from 100 to 200 mg/kg body weight. Control mice received 300 μl citrate buffer alone. Duplicate glucose measurements were performed on whole venous blood collected from the tail vein of non-fasting animals at 48 h after STZ treatment and twice weekly thereafter, using the Freestyle Flash Blood Monitoring System (Nipro, Tokyo, Japan) according to the manufacturer's instructions. For investigation of the effect of STZ concentration on ES cell differentiation, 12 mice were used. Mice received ES cells 24 h after STZ injection by i.p. administration. All ES cells were injected on the same day and from the same cell preparation. The cell injection site was the lower abdomen, as far from the pancreas as possible. Physiological sample data at day 14 for these animals is shown in Table 1. For renal capsule transplantation experiments, 1×10^6 ES cells were transplanted 24 h following treatment of mice with 150 mg/kg STZ (n=2) or citrate buffer (n=2). Briefly, recipient mice were anaesthetised by exposure to 1–3% isoflurane, and a 1.5-cm cut through the skin and muscle of the left flank

Table 1 Physiological characteristics of animals transplanted i.p. with mouse embryonic stem cells

STZ treatment	Blood glucose (mmol/l)[a,b]	Weight (g)[a]	ES homing to pancreas?[a]
Citrate buffer #1	4.2	21.6	No
Citrate buffer #2	4.4	20.4	No
Citrate buffer #3	5.0	21.9	No
STZ 100 mg/kg #1	6.6	23.3	No
STZ 100 mg/kg #2	6.7	21.6	No
STZ 100 mg/kg #3	6.2	22.8	No
STZ 150 mg/kg #1	6.2	20.2	Yes
STZ 150 mg/kg #2	4.9	21.2	Yes
STZ 150 mg/kg #3	5.0	20.2	Yes
STZ 200 mg/kg #1	8.7	20.5	Yes
STZ 200 mg/kg #2	21.7	17.3	Yes
STZ 200 mg/kg #3	19.6	17.4	Yes

Relationship between STZ dose, blood glucose concentration (>11.1 mmol/l=hyperglycaemic) and effect on homing to the pancreas of transplanted mouse ES cells measured by in vivo imaging. Representative data is shown for mice at day 14. Blood glucose concentration remained similar to day 14 values for each animal until mice were killed on day 24. Average weight of mice at day 0=19±1 g.

[a] At day 14 post-treatment

[b] Average of two consecutive readings

dorsal to the spleen was made. The exposed wound was flushed with 1 ml PBS containing penicillin/streptomycin (Invitrogen, Carlsbad, CA, USA) and the kidney was pushed through the wound. A small cut was made laterally on the kidney membrane using a scalpel, and 10 μl PBS containing 1×10^6 ES cells was gently expelled towards the bottom of the kidney capsule using a 20-μl pipette tip. The kidney was replaced in the abdominal cavity, and the incision was closed with small wound clips. For i.v. transplantation, 1×10^6 ES cells in 100 μl PBS were injected via the tail vein 24 h after STZ treatment. For evaluation of induction of hormone-positive duct cells in the pancreas of STZ-treated mice, animals were treated with citrate buffer (group 1, n=3), 150 mg/kg STZ (group 2, n=6) or 200 mg/kg STZ (group 3, n=6), and killed 24, 48 and 72 h later (one in group 1, two in group 2, three in group 3 for each time point), and tissues were sectioned and stained for glucagon and insulin.

For estimation of permanent beta cell depletion in 150 mg/kg STZ- vs citrate buffer-injected mice, six animals were used. Mice were treated with 150 mg/kg STZ (n=3) or citrate buffer (n=3) and killed after 24 days, then pancreas sections were double-stained using immunofluorescence for glucagon and insulin as described below. All six mice had blood glucose concentrations <11.1 mmol/l throughout the 24-day period. Islets containing between 10 and 400 cells for each animal were photographed, and alpha and beta cells were counted using ImageJ software (version 1.31v) available from http://rsb.info.nih.gov/ij/download.html, last accessed in July 2006. For each islet, the ratio of beta:alpha cells was calculated and averaged for >30 islets per mouse (100 islets per group). For evaluation of the percentage of ES cell tumours occupied by pancreatic foci and PDX-1-positive foci ImageJ software was used to draw a closed perimeter around the foci and measure the sum of the areas occupied by these foci relative to the area of a closed perimeter drawn around the whole tissue section. This was repeated for several tissue sections from each mouse and averaged. For estimation of numbers of insulin-positive and PDX-1/insulin double-positive cells, individual cells were counted within the closed perimeter area of the ES cell tumour pancreatic foci only and their overall ES cell tumour proportion was then estimated.

Culture and in vivo transplantation of ES cells

The firefly luciferase-expressing ESJ1 cell line, a J1 cell clone of 129SV male origin, was established as described previously [11]. Twenty-four hours after STZ treatment, mice received 1×10^6 ES cells by single i.p. injection in 300 μl PBS prepared as described previously [11]. In vivo imaging analysis of transplanted ES cells was conducted in a cryogenically cooled IVIS system (Xenogen, Alameda, CA, USA). Mice were administered D-luciferin (150 mg/kg; Promega, Madison, WI, USA) by i.p. injection and anaesthetised by exposure to 1–3% isoflurane. Photons from animal whole bodies were counted 10 min later using the IVIS imaging system according to the manufacturer's instructions, and data were analysed using LIVINGIMAGE 2.50 software (Xenogen). The amount of light generated was directly related to the amount of luciferase-producing cells. The development of pancreatic ES cell tumours was monitored twice weekly.

Immunofluorescence and immunohistochemical analyses

Following killing of mice by cervical dislocation, pancreases and ES cell tumour tissues were preserved in 10% formalin solution, before being embedded in paraffin and sectioned. Sections were deparaffinised in xylene and rehydrated through a graded ethanol series. Antigen retrieval was performed by boiling sections for 5 min in 10 mmol/l citrate buffer followed by cooling for 30 min to room temperature. Blocking was carried out using Image-iT FX Signal Enhancer (Invitrogen) for 30 min at room temperature. Primary antibodies were applied overnight at 4°C. AlexaFluor secondary antibodies (1:1,000; Invitrogen) were applied for 30 min at room temperature. All antibodies were diluted in ChemMate Antibody Diluent (Dako, Kyoto, Japan). Immunofluorescence-stained sections were mounted with Vectashield mounting medium (Vector Laboratories, Burlingame, CA, USA) containing 4′, 6-diamidino-2-phenylindole (DAPI) to visualise nuclei. The following primary antibodies were used: anti-insulin (1:400, #MAB1417; R&D systems, Minneapolis, MN, USA), anti-glucagon (1:200, #sc-7779; Santa Cruz Biotechnology, Santa Cruz, CA, USA), anti-C-Peptide (1:400, #4023-01; Linco, St Charles, MO, USA), anti-HNF3β (1:100, #sc-9187; Santa Cruz) anti-PDX-1 (1:100, #07-696; Upstate, Charlottesville, VA, USA), anti-α-amylase (1:200, #A8273; Sigma) and anti-luciferase (1:100, #PM016; MBL, Woburn, MA, USA). Luciferase, HNF3β and α-amylase staining was performed using the Vectastain ABC kit (Vector Laboratories) according to the manufacturer's instructions, followed by haematoxylin or eosin counter-staining using standard methods.

Results

Beta cell neogenesis following STZ treatment

Doses of 150 mg/kg STZ or below consistently failed to induce overt hyperglycaemic blood glucose concentrations (>11.1 mmol/l) up to 4 weeks following treatment (Table 1; sample data is shown at day 14), while doses of 200 mg/kg

usually led to acute hyperglycaemia (blood glucose concentration >11.1 mmol/l) within 48 h, which was accompanied by sustained poor weight gain and polyuria thereafter. The lowest single STZ dose that can induce hyperglycaemia in mice is variable and dependent on genetic background for inbred strains. The BALB/c genetic background displays unusually high resistance to STZ-induced DNA damage, which is directly related to poly (ADP-ribose) polymerase (PARP) activation and NAD depletion [12]. This would explain why a STZ dose of 150 mg/kg, which is sufficient to induce rapid hyperglycaemia in some mouse strains, did not do so in this study. Nevertheless, since STZ degrades rapidly and mice treated with 150 mg/kg STZ did not develop elevated blood glucose levels in this study, an alternative method was necessary to establish that the STZ dose administered in this instance induced some degree of beta cell depletion. As STZ is a selective destroyer of beta cells, the alpha cell population should remain constant before and after treatment (unless there is an expansion of alpha cells during regeneration that has not previously been demonstrated). We therefore compared the average ratio of beta (insulin-positive): alpha (glucagon-positive) cells over a range of islet sizes from non-ES cell-transplanted control mice (n=3) and mice treated with 150 mg/kg STZ (n=3) 24 days after treatment. Using this approach we estimated that the average rate of permanent destruction of beta cells in euglycaemic mice treated with 150 mg/kg was 50% (Fig. 1). Between 24 and 48 h after 150 mg/kg STZ treatment, some ductal hormone-positive cells were detectable in the pancreas of treated mice, including occasional insulin/glucagon double-positive cells (data not shown). However, 24 days after treatment, hormone-positive duct cells were not detectable. In contrast, in hyperglycaemic mice treated with 200 mg/kg STZ, clusters of insulin-positive cells within the pancreatic ducts were common after 24 days (data not shown), as previously observed in the regenerating adult pancreas under hyperglycaemic conditions [13].

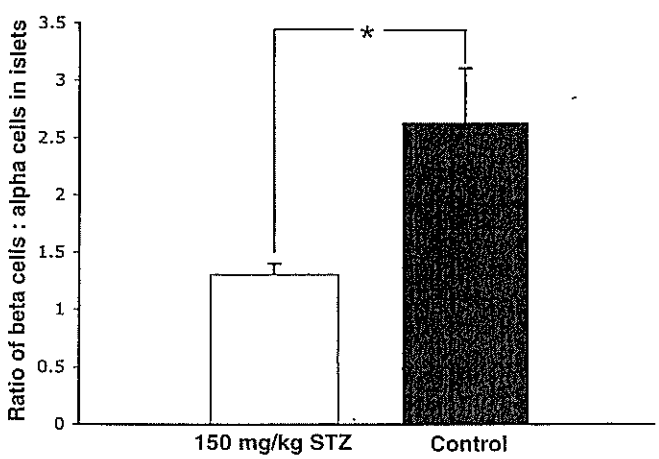

Fig. 1 Permanent beta cell depletion in the pancreatic islets of euglycaemic mice treated with STZ. Mice received 150 mg/kg STZ (*white bar*; n=3) or citrate buffer alone (*black bar*; n=3). The average ratio of beta (insulin-positive):alpha (glucagon-positive) cells in >100 islets per group at day 24 after STZ treatment revealed approximately 50% permanent beta cell depletion. Data are presented as means±SEM. *p<0.05, t test

Transplanted ES cells migrate to and proliferate in the STZ-injured pancreas

Pancreatic homing and proliferation of i.p. transplanted ES cells was clearly detectable by in vivo imaging in all animals that received doses of 150 mg/kg or 200 mg/kg STZ from day 14 after transplantation (Fig. 2). At lower STZ doses (100 mg/kg) and in citrate buffer-treated mice, homing to the pancreas was not detected in any animals up to day 24 when all mice were killed. Earlier attempts using i.v. transplantation of ES cells also gave rise to small peri-pancreatic tumours. However, these tumours developed more slowly than following i.p. transplantation (Electronic supplementary material [ESM] Fig. 1) and mice were prone to lethal pulmonary teratomas. All mice produced s.c. tumours at the site of injection, presumably due to some leaking of cells into the s.c. space during ES cell injection. In addition to s.c. tumours, small teratomas were occasionally observed at random sites (non-pancreas-associated) sites in the peritoneum of i.p. ES cell transplanted mice. Anatomical analysis of the pancreata of 150 mg/kg STZ-treated mice following killing at 24 days after ES cell injection revealed vascular networks interconnecting ES cell-derived tumour nodules with the vasculature of the host pancreas (Fig. 2), indicating that the movement of soluble factors between pancreas and ES cell tumour was facilitated during ES cell tumour growth and differentiation.

Transplanted ES cells differentiate into hormone-positive cell clusters in STZ-treated mice

ES cell-derived pancreatic tumours were analysed for expression of hormonal markers of pancreatic islet (alpha and beta) cells. Staining of serial ES cell tumour sections alternately for insulin and glucagon revealed foci with clusters of hormone-positive cells spatially associated with each other and arranged along the periphery of rosettes of large eosinophilic granular cells, which displayed histological similarity to pancreatic acini (Fig. 3c, inset). These acinar-like cells were hormone-negative. In addition, these ES cell tumour foci always contained lumenal columnar epithelium adjacent to the hormone-positive clusters. This epithelium showed weak hormone staining that was polarised towards the acinar-like and hormone-positive cell clusters and occasionally contained cells that stained strongly positive for glucagon or insulin (Fig. 3, arrowheads).

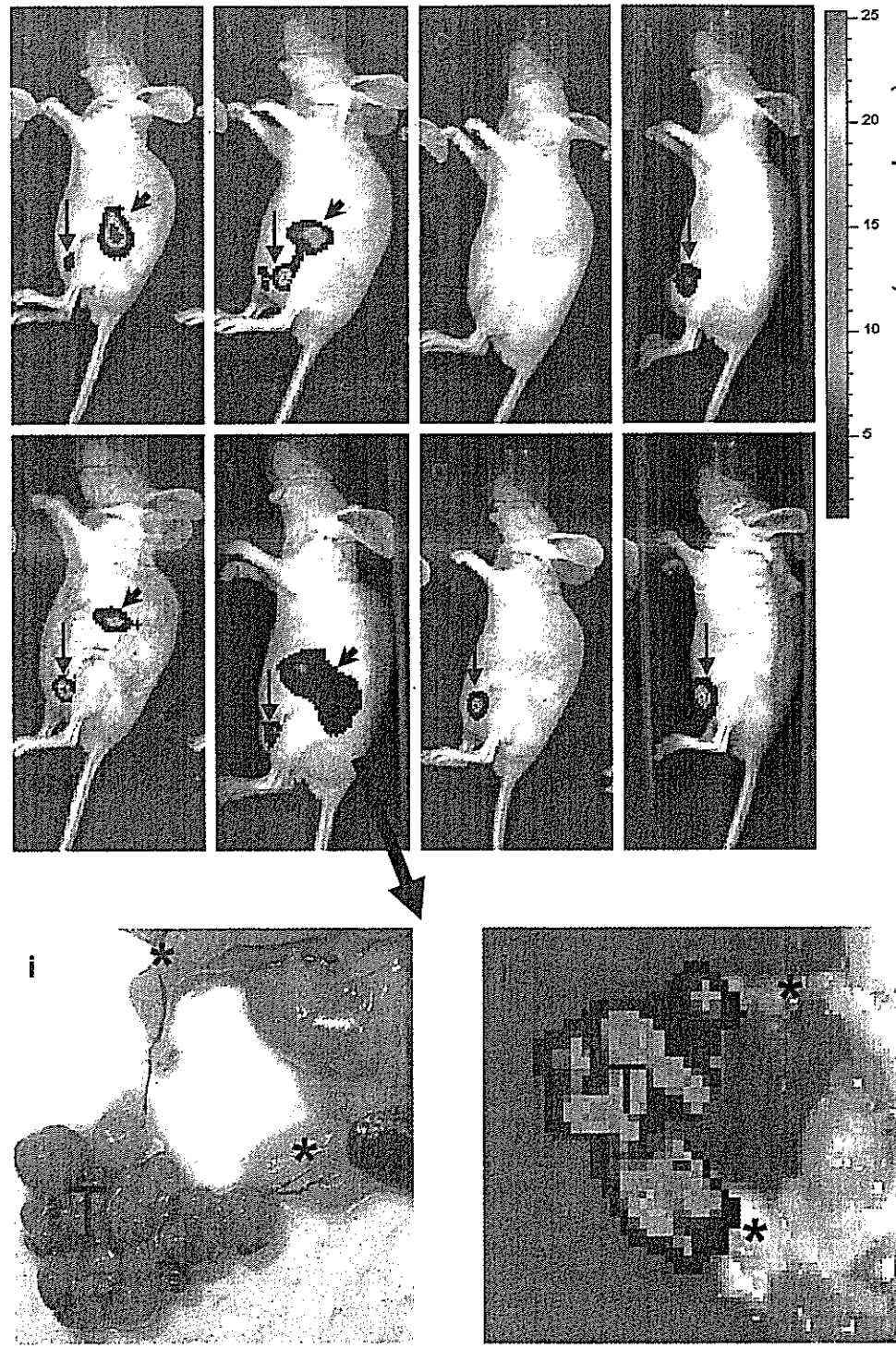

Fig. 2 Pancreatic homing and expansion of ES cells in STZ-treated mice were monitored in vivo by bioluminescent imaging using the IVIS system. Day 14 (**a–d**) and day 24 (**e–h**) representative images of nude mice injected i.p. on day 0 with STZ at 200 mg/kg (**a**, **e**), 150 mg/kg (**b**, **f**), 100 mg/kg (**c**, **g**) or citrate buffer only (**d**, **h**), followed 24 h later by i.p. injection of 1×10^6 ES cells in 300 μl Dulbecco's PBS are shown; pancreas-associated ES cell tumours are indicated by arrowheads; all mice developed s.c. ES cell tumours at injection site (*arrows*). **i** At day 24, 150 mg/kg STZ dose, highly vascularised ES cell tumour nodules (T) were interconnected with the host pancreas vasculature (*). **j** confirmation of ES cell homing to pancreas by ex vivo imaging

Insulin-positive cell clusters are associated with α-amylase-positive acinar cells in ES cell tumour foci, suggesting a common origin

Closer analysis of ES cell tumour foci revealed that insulin-positive cell clusters were located in close contact with α-amylase-positive acinar-like cells (Fig. 4). However, there was no overlap between α-amylase and insulin staining. The occurrence of endocrine and exocrine cells at common foci suggests that they originated from a common precursor cell type. Approximately 0.1% of the peri-pancreas teratomas comprised pancreatic foci that we define as cell clusters containing lumenal epithelial cells positive for α-amylase, insulin and PDX-1 in close association (Table 2). Furthermore, this tight arrangement of cells with distinguishable specialised functions is similar to that found

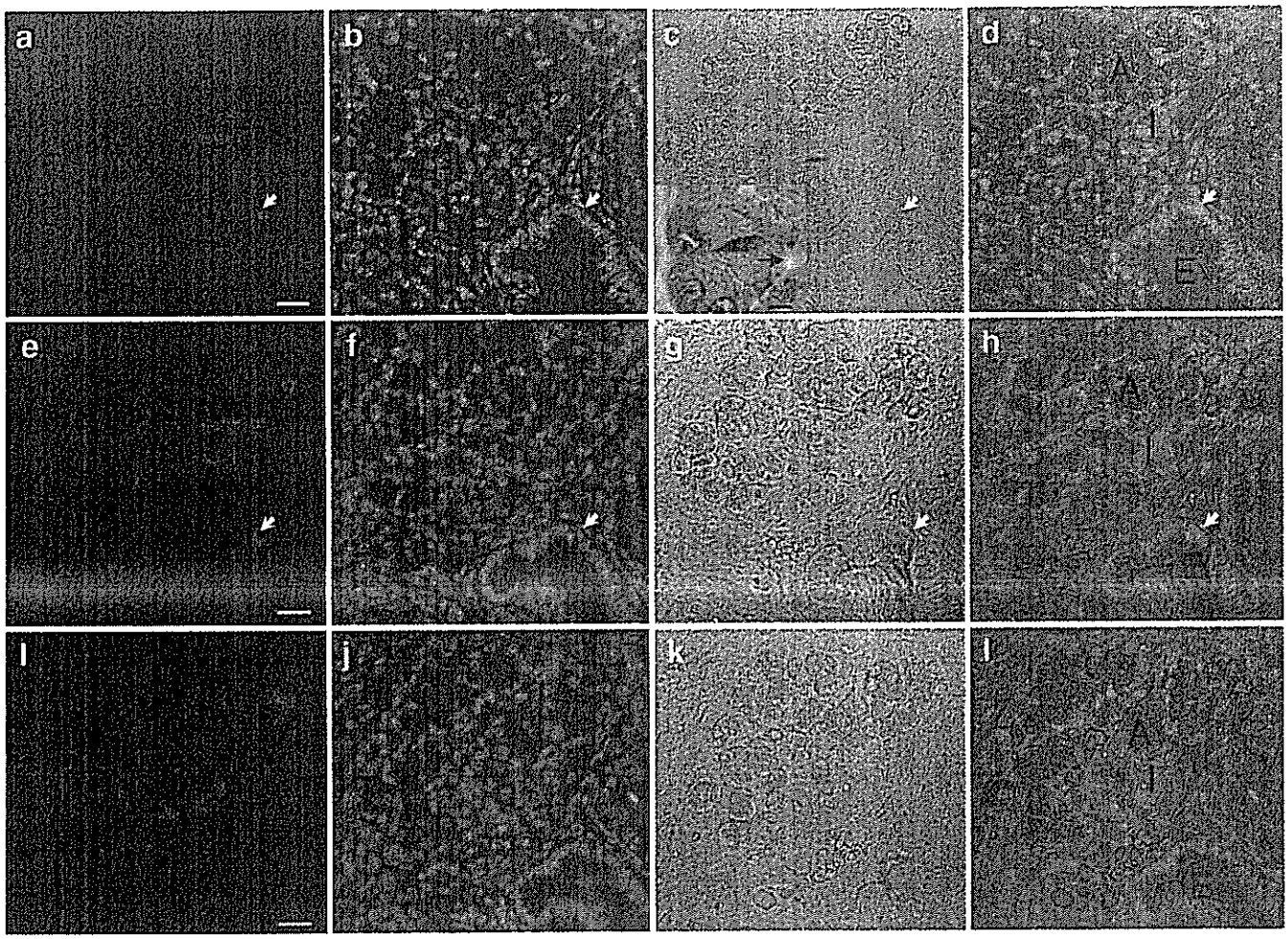

Fig. 3 Hormone-positive clusters are induced in ES cell tumours following 150 mg/kg STZ treatment. Serial sections of ES cell tumour foci were stained alternately for glucagon (*red*; **a–d**, **i–l**) and insulin (*red*; **e–h**). Hormone-positive cells were observed within the lumenal epithelium (E, *arrowheads*) and in adjacent islet-like clusters (I). In close proximity to the islet-like clusters were clusters of large granular cells with acinar-like cell morphology (A). **c** Inset (scale bar=5 μm) shows a haematoxylin and eosin photomicrograph of a segment of an ES cell tumour acinus. The pyramidal cell shape with nucleus at broad basal surface and eosinophilic zymogen granules in the apical cytoplasm towards the lumen (*arrow*) are clearly seen. **a**, **i** Glucagon; **e** insulin; **b**, **f**, **j** DAPI; **c**, **g**, **k** phase contrast; **d**, **h**, **l** hormone/DAPI/phase contrast overlay. Scale bar=25 μm

in maturing islets and acini in the pancreas post embryonic day (E) 14.5, and occurred in proximity to simple columnar epithelium resembling endodermal gut epithelium.

ES cell tumour foci contain PDX-1-positive epithelium resembling pancreatic anlage

PDX-1 is the earliest marker of pancreatic stem cells that give rise to all three pancreatic lineages [14] and is essential for pancreatic morphogenesis. It is expressed almost uniformly in the dorsal and ventral pancreatic buds that evaginate from the ventral gut epithelium. Following lineage commitment, PDX-1 expression is lost in pancreas cells, and is re-expressed at high levels in mature beta cells as a key transactivator of beta cell-specific hormone expression. PDX-1 staining of lumenal epithelium in ES cell tumour foci revealed a high density of positive cells (50%) (Fig. 5a). The PDX-1-positive epithelium was hormone- and α-amylase-negative, and displayed polarisation with distinct tracts of uniformly PDX-1-positive cells distinguishable from PDX-1-negative epithelial cells. Co-staining of foci for α-amylase revealed that this polarity was towards exocrine-like cells, which arose as a continuum of the PDX-1-positive epithelium, with a clear down-regulation of PDX-1 at the interface with cells undergoing induction of the gene for α-amylase. The α-amylase-positive cells were PDX-1-negative. We confirmed that PDX-1-positive foci originated from the endodermal lineage by co-staining for HNF3β (Fig. 5h). To determine whether ES cell tumours could undergo pancreatic morphogenesis in another well-vascularised location, we transplanted undifferentiated ES cells under the kidney capsule of 150 mg/kg STZ- (n=2) and citrate buffer-treated (n=2) mice (ESM Fig. 2). Approximately 2% of the kidney

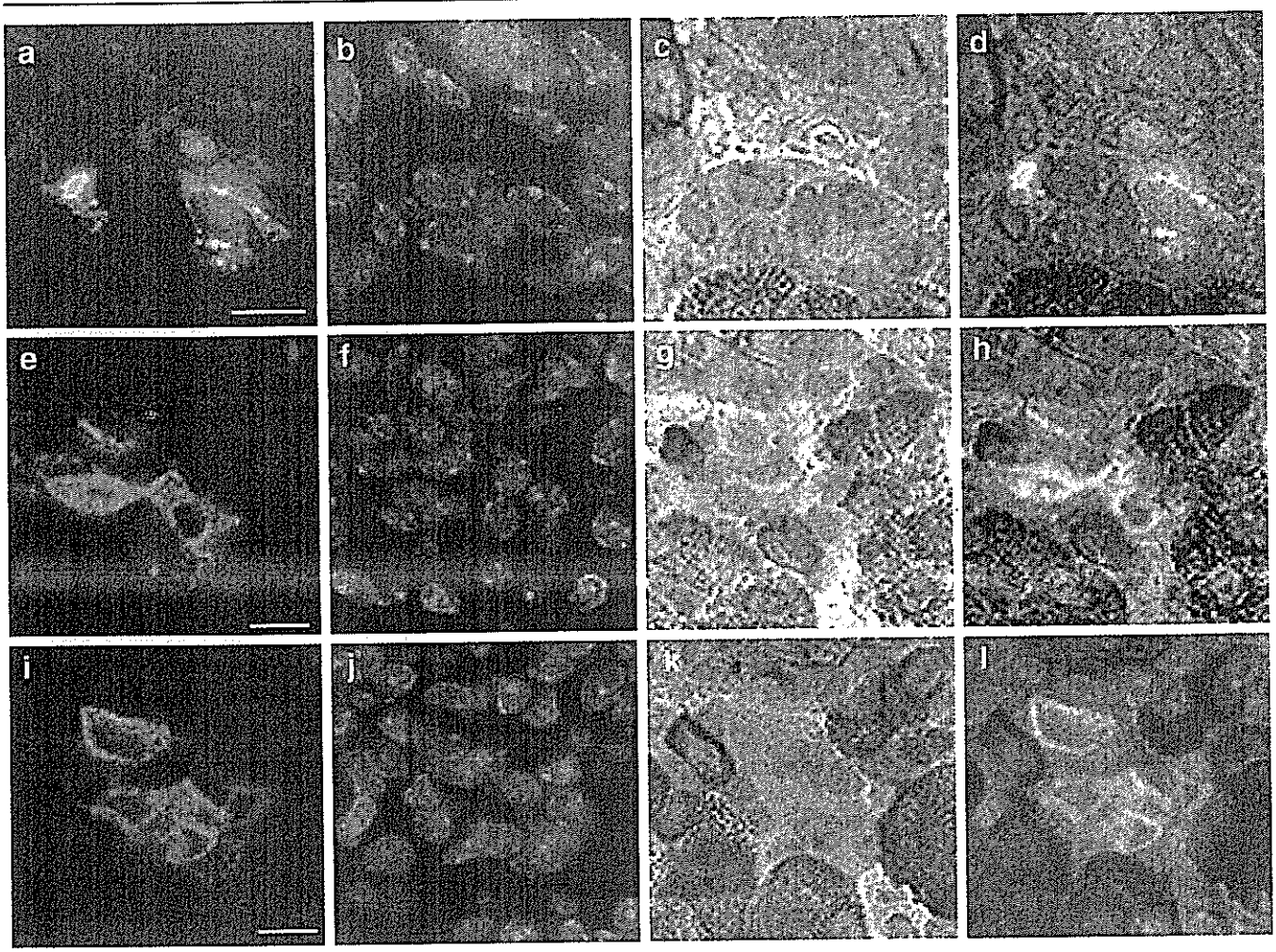

Fig. 4 Induction of beta cell-like clusters in ES cell tumour foci appears to follow a developmental pathway. Serial sections of tumour foci were stained for insulin (*green*) and α-amylase (*brown*). Clusters of insulin-positive cells appear in close association with α-amylase-positive acinar cells without overlap of marker expression. This arrangement is similar to that found in the later stages of pancreatic organogenesis (after E 14.5). **a**, **e**, **i** Insulin; **b**, **f**, **j** DAPI; **c**, **g**, **k** α-amylase; **d**, **h**, **l** insulin/DAPI/α-amylase overlay. Scale bars=5 μm

capsule ES cell tumour from the 150 mg/kg STZ-treated mice contained polarised PDX-1-positive luminal epithelium (ESM Fig. 3), compared with 0.1% of citrate buffer-treated mice (data not shown).

Table 2 Proportion of peri-pancreas ES tumours expressing pancreas-associated proteins

Immunohistochemical marker	Percentage of peri-pancreas tumour
HNF3β	15±2.1
PDX-1	1.4±0.11
PDX-1/insulin/α-amylase[a]	0.1±0.022
PDX-1/insulin[b]	0.01±0.003

Data at day 24 following ES transplantation. Tumours from three mice were evaluated. Data is presented±SD. Peri-pancreas ES tumours expressing pancreas-associated proteins also expressed luciferase.
[a] Foci containing cells representing all three markers, either single- or double-positive. Average number of foci per tumour section=2
[b] Double-positive cells

ES cell tumour foci contain mature beta cells

To further characterise the pancreatic cells of our ES cell tumour foci we performed double-staining for C-peptide/PDX-1, insulin/PDX-1 and glucagon/PDX-1. During development, the majority of early insulin cells do not express PDX-1 when they first appear, but PDX-1 is later upregulated in the mature beta cells [15]. However, mature alpha cells, which are interspersed with beta cells in the mature islet, are PDX-1-negative. Figure 6a–h illustrates a strong PDX-1/insulin/C-peptide triple-positive mature beta cell located in an ES cell tumour focus but separate from the PDX-1-positive epithelium. Glucagon-positive putative alpha cells were PDX-1-negative but adjacent to PDX-1-positive cells (beta cells) in a similar arrangement to that found in pancreatic islets. To confirm that the ES cell tumour-derived beta cells were derived from the endodermal lineage, we demonstrated nuclear co-expression of the

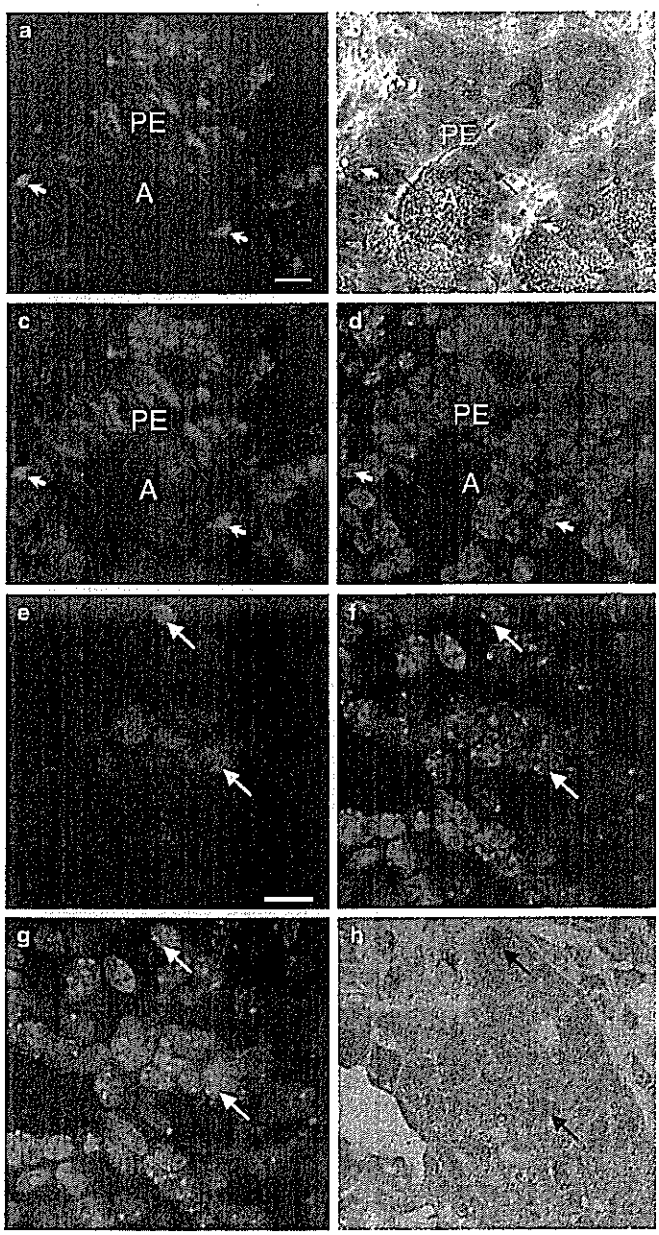

Fig. 5 **a–d** PDX-1 (*green*) is expressed in the nuclei of 50% of lumenal epithelial cells in ES cell tumour pancreatic foci. PDX-1-positive luminal epithelium is usually hormone-negative and is polarised towards α-amylase-positive (*brown*) acinar cells (A) which can be seen emerging as a continuum from the PDX-1-positive epithelium (PE) and cells at the interface show downregulation of PDX-1 expression (*arrows*). PDX-1-positive cells are also located outside the luminal epithelium (*arrowheads*). These cells are insulin-positive (not shown). **a** PDX-1; **b** α-amylase; **c** PDX-1/DAPI overlay; **d** DAPI. Scale bar=10 μm. **e–h** Co-localisation of PDX-1 and HNF3β proteins in pancreatic foci in ES cell tumours confirms their endodermal lineage. Sections of peri-pancreas tumours were stained for PDX-1 (*red*) and HNF3β (*brown*), both revealing nuclear localisation. Examples of double-positive cells are indicated by arrows. **e** PDX-1; **f** DAPI; **g** PDX-1/DAPI overlay; **h** HNF3β. Scale bar=10 μm

HNF3β protein with PDX-1 and insulin (Fig. 6m–q). Finally, tissue sections were co-stained for luciferase along with glucagon and insulin to demonstrate that the hormone-positive cells observed in the ES cell tumours were indeed derived from the transplanted cells (Fig. 6r–v).

Discussion

The pancreas appears to lack the ability to sense its size, unlike the liver, and regeneration following pancreatectomy is incomplete [16]. Nevertheless, the observation that a range of stimuli can increase growth of acini [4, 17], ducts [5] and beta cells [2] suggests that there must be local signals capable of promoting growth in the postnatal animal. Following STZ treatment, irrespective of whether a high or low dose is used, beta cell replenishment is incomplete [9], which raises the possibility that regenerating signals are present but the pancreas is incapable of an effective response.

We demonstrated here that when ES cells were introduced to mice with partial STZ-induced beta cell ablation, the cells migrated to the pancreas and proliferated, forming highly vascularised tumour nodules whose vasculature was connected to that of the host pancreas. These nodules contained cells with characteristics of endocrine (alpha and beta cells) and exocrine (α-amylase-positive) cells, indicating that regenerative signals produced by the injured pancreas are capable of stimulating organ morphogenesis from precursor PDX-1-positive endodermal epithelium. This provides a clear demonstration, for the first time, that pancreatic beta cell ablation in the absence of hyperglycaemia in the adult produces soluble signals that can recapitulate elements of embryonic pancreatic development.

In the mouse embryo, the pancreatic primordium is first visible at E 9.5 as an evagination of the foregut endoderm, consisting of a highly folded epithelial sheet with apical and basal surfaces continuous with those of the gut tube [18]. At this stage most of the cells express PDX-1, the master regulator of pancreas development [14], and glucagon-positive cells can be detected, although these first glucagon-positive cells are post-mitotic and do not contribute to the final alpha cell pool [18]. One day later, insulin-positive cells appear, and over the next 2–3 days, cells are frequently found to express both hormones together [19]. However, alpha and beta cells appear to be derived independently in the mouse pancreas [20]. At around E 14.5, exocrine cells become distinguishable from endocrine cells [18]. Endocrine cells are largely individual and associated with the ducts until the end of gestation (about E 18.5), when they are found as islets [18].

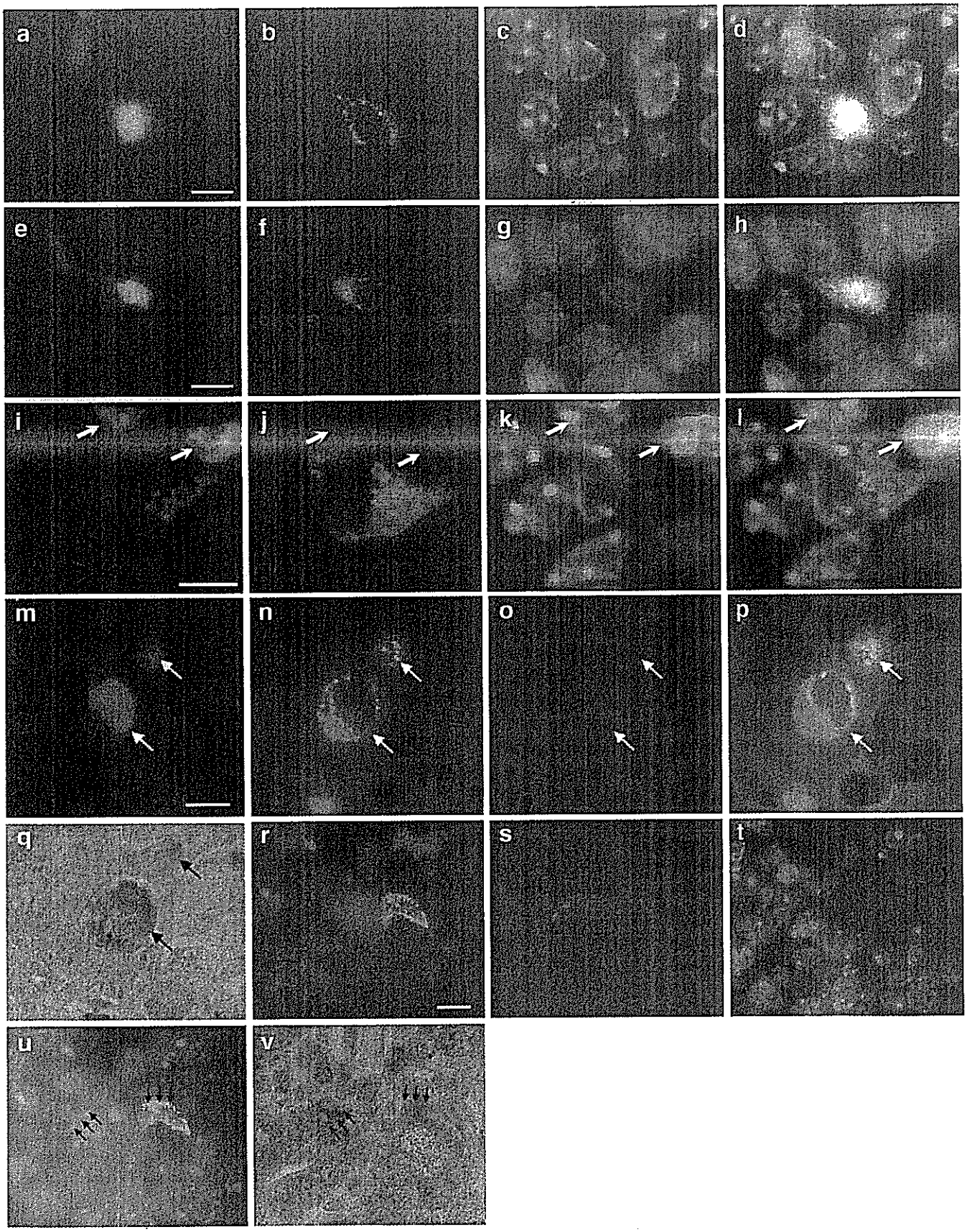
a
b
c
d
e
f
g
h
i
j
k
l
m
n
o
p
q
r
s
t
u
v

◀ **Fig. 6** Mature beta and alpha cells are found in ES cell tumour pancreatic foci. **a–d** and **e–h** represent serial sections. **a–d** and **i–l** represent the same tissue section. **a–c** PDX-1 (*green*), C-peptide (*red*), DAPI (*blue*); **d** PDX-1/C-peptide/DAPI overlay; **e–g** PDX-1 (*green*), insulin (*red*), DAPI (*blue*); **h** PDX-1/insulin/DAPI overlay; **i–k** PDX-1 (*green*), glucagon (*red*), DAPI (*blue*); **l** PDX-1/glucagon/DAPI overlay showing a PDX-1-negative/glucagon-positive cell adjacent to PDX-1-positive/glucagon-negative beta cells (*arrows*) — both cell types have characteristics of mature pancreatic islet cells. Scale bars=5 μm. **m–q** Mature beta cells in ES cell tumours are induced from the endodermal lineage. HNF3β co-localises with PDX-1 in the nuclei of insulin-positive cells (*arrows*). **m** PDX-1; **n** insulin; **o** DAPI; **p** PDX-1/insulin/DAPI overlay; **q** HNF3β. Scale bar=5 μm. **r–v** Hormone-expressing cells in ES cell tumour pancreatic foci are induced from the transplanted cells. Luciferase staining is co-localised in hormone-expressing cells (*arrows*) from peri-pancreas ES cell tumour sections. **r** insulin (*green*); **s** glucagon (*red*); **t** DAPI (*blue*); **u** insulin/glucagon/DAPI overlay; **v** luciferase (*brown*). Scale bar=10 μm

The presence of PDX-1-positive lumenal epithelium, hormone-positive cell clusters and pancreatic acini in ES cell tumours indicates that the insulin-positive cells most likely arose from pancreas morphogenesis and not merely by cytodifferentiation. Additional support for this conclusion comes from both tissue reconstitution and genetic experiments [21–23] that have definitively demonstrated that pancreatic mesenchyme is required for exocrine, but not endocrine, differentiation. Subcutaneous ES cell tumours that formed at the ES cell injection site in both STZ-treated and non-treated mice revealed no evidence of pancreatic differentiation (data not shown), indicating that factors produced by the regenerating pancreas were required for the ES cell differentiation and suggesting that these factors may be more effective at close range.

In the pancreas itself, we observed evidence of inefficient beta cell neogenesis in 150 mg/kg STZ-treated animals, indicated by islets with altered beta:alpha cell ratios, as compared with control mice 24 days after treatment. Approximately half of islet beta cells were permanently lost following this treatment regimen. Although we have not measured the rate of insulin production in these injured islets, we found that normal glucose levels were maintained throughout a 24-day period. However, increasing the STZ dose to 200 mg/kg almost invariably induced rapid hyperglycaemia, suggesting that 150 mg/kg animals were close to exhibiting pathological blood glucose levels. In the present study our aim was to separate the secondary effects of high blood glucose, a known inducer of beta cell neogenesis, on its own in the absence of beta cell damage [24] from the primary effects of beta cell loss. Fernandes et al. [25] found that while a key subpopulation of intra-islet somatostatin/PDX-1 double-positive transitionary cells were expanded in mice following high-dose STZ treatment, low doses of STZ did not induce beta cell neogenesis, suggesting that the neogenic response observed at high STZ doses was dependent on or related to elevated blood glucose levels. The rate of pancreatic foci and PDX-1/insulin double-positive cells was similar in peri-pancreas ES cell tumours from 200 mg/kg-treated mice (data not shown). However, since these mice were mildly hyperglycaemic (<22.2 mmol/l) we cannot yet remark on the effect of higher blood glucose concentrations (>22.2 mmol/l), nor the possibility of glucose-induced regenerative stimuli obscuring a reduction in beta cell loss-induced regenerative stimuli caused by the higher STZ doses required for induction of severe hyperglycaemia. That euglycaemic STZ-treated mice induced neogenesis of multiple lineages—islet and acinar—in exogenous multipotent cells strongly suggests that STZ-mediated beta cell damage, in the absence of hyperglycaemia, produces pancreas regeneration signals, although they apparently have limited effect in the adult pancreas itself since beta cell loss by the same STZ dose is never fully replenished. Our data raises the possibility that this lack of self-regeneration may be due to a limitation of the organ to respond to signals rather than an absence of regenerating stimuli per se. While it is unlikely that pancreatic morphogenesis depends on cell fusion between ES and host stem cells in this model, it cannot yet be ruled out that cell fusion events may occur that involve host cells such as macrophages, which are known to be relatively abundant in nude mice.

In conclusion, by uncoupling the regenerative signal produced by the damaged pancreas from the regenerative response, the model described here recapitulates elements of embryonic pancreas development in the injured adult pancreas. Future studies will focus on identification of factors produced by the injured pancreas. In addition, it will be important to characterise the response of putative adult beta stem cell types, such as bone marrow-derived mesenchymal stem cells [26] and intra-pancreatic stem cells [27, 28], to stimuli produced by the STZ-injured pancreas. This may be a valuable system for understanding the mechanisms of beta cell neogenesis in the adult and for identification of regenerative factors for use in tissue engineering in vitro.

Acknowledgements We thank S. Kume (Institute of Molecular Embryology and Genetics, Kumamoto University) for manuscript review and scientific advice and N. Isohata (Genetics Division, NCCRI) and A. Inoue (Section for Studies on Metastasis, NCCRI) for technical assistance. This work was supported in part by a Grant-in-Aid for the Third-Term Comprehensive 10-Year Strategy for Cancer Control; Health Science Research Grants for Research on the Human Genome and Gene Therapy from the Ministry of Health, Labour, and Welfare of Japan; the Program for Promotion of Fundamental Studies in Health Sciences of the National Institute of Biomedical Innovation (NiBio).

Duality of interest The authors state that they have no duality of interest.

References

1. The Diabetes Control and Complications Trial Research Group (1997) Hypoglycemia in the Diabetes Control and Complications Trial. Diabetes 46:271–286
2. Gu D, Sarvetnick N (1997) Epithelial cell proliferation and islet neogenesis in IFN-γ transgenic mice. Development 118:33–46
3. Chang AY, Diani AR (1985) Chemically and hormonally induced diabetes mellitus. In: Volk BW, Arquilla ER (eds) The diabetic pancreas, 2nd edn. Plenum, New York, pp 415–438
4. Elsasser HP, Biederbick A, Hern HF (1994) Growth of rat pancreatic acinar cells quantitated with a monoclonal antibody against the proliferating cell nuclear antigen. Cell Tissue Res 276:603–609
5. Rosenberg L, Brown RA, Duguid WP (1983) A new approach to the induction of duct epithelial hyperplasia and nesidioblastosis by cellophane wrapping of the hamster pancreas. J Surg Res 35:63–72
6. Like AA, Rosini AA (1976) Streptozotocin-induced pancreatic insulitis: new model of diabetes mellitus. Science 193:415–417
7. Brosky G, Logothetopoulos J (1969) Streptozotocin diabetes in the mouse and the guinea pig. Diabetes 18:606–611
8. Steiner H, Oelz O, Zahnd G, Froesch ER (1970) Studies on islet cell regeneration, hyperplasia and intrainsular cellular interactions in long lasting streptozotocin diabetes in the rat. Diabetologia 6:558–564
9. Bonner-Weir S, Trent DF, Honey RN, Weir GC (1981) Responses of neonatal rat islets to streptozotocin. Diabetes 30:64–69
10. Yamamoto H, Quinn G, Asari A et al (2003) Differentiation of embryonic stem cells into hepatocytes: biological functions and therapeutic application. Hepatology 37:983–993
11. Teratani T, Yamomoto H, Aoyagi K et al (2005) Direct hepatic fate specification from mouse embryonic stem cells. Hepatology 41:836–846
12. Cardinal JW, Allan DJ, Cameron DP (1999) Poly(ADP-ribose) polymerase activation determines strain sensitivity to streptozotocin-induced beta cell death in inbred mice. J Mol Endocrinol 22:65–70
13. Bonner-Weir S (2000) Islet growth and development in the adult. J Mol Endocrinol 24:297–302
14. Jonsson J, Carlsson L, Edlund T, Edlund H (1994) Insulin-promoter-factor 1 is required for pancreas development in mice. Nature 371:606–609
15. Ohlsson H, Karlsson K, Edlund T (1993) IPF1, a homeodomain-containing transactivator of the insulin gene. EMBO J 12:4251–4259
16. Lehv M, Fitzgerald PJ (1968) Pancreatic acinar cell regeneration. IV. Regeneration after surgical resection. Am J Pathol 53:513–535
17. Jensen JN, Cameron E, Garay MVR, Starkey TW, Gianani R, Jensen J (2005) Recapitulation of elements of embryonic development in adult mouse pancreatic regeneration. Gastroenterology 128:728–741
18. Slack JMW (1995) Developmental biology of the pancreas. Development 121:1569–1580
19. Madsen OD, Jensen J, Blume N et al (1996) Pancreatic development and maturation of the islet β cell. Eur J Biochem 242:435–445
20. Jensen J, Heller R, Funder-Nielsen T et al (2000) Independent development of pancreatic α- and β-cells from neurogenin3-expressing precursors. Diabetes 49:163–176
21. Ahlgren U, Pfaff SL, Jessell TM, Edlund T, Edlund H (1997) Independent requirement for ISL1 in formation of pancreatic mesenchyme and islet cells. Nature 385:257–260
22. Wessells N, Cohen J (1966) Early pancreatic organogenesis: morphogenesis, tissue interactions, and mass effects. Dev Biol 15:237–270
23. Rose M, Crisera C, Colen K, Connelly PR, Longaker M, Gittes G (1999) Epithelio-mesenchymal interactions in the developing pancreas: morphogenesis of the adult architecture. J Pediatr Surg 34:774–779
24. Lipsett M, Finegood DT (2002) β-Cell neogenesis during prolonged hyperglycemia in rats. Diabetes 51:1834–1841
25. Fernandes A, King LC, Guz Y, Stein R, Wright CVE, Teitelman G (1997) Differentiation of new insulin-producing cells is induced by injury in adult pancreatic cells. Endocrinology 138:1750–1762
26. Sordi V, Malosio ML, Marchesi F et al (2005) Bone marrow mesenchymal stem cells express a restricted set of functionally active chemokine receptors capable of promoting migration to pancreatic islets. Blood 106:417–427
27. Seaberg RM, Smukler SR, Kieffer TJ et al (2004) Clonal identification of multipotent precursors from adult mouse pancreas that generate neural and pancreatic lineages. Nat Biotechnol 22:1115–1124
28. Hao E, Tyrberg B, Itkin-Ansari P et al (2006) Beta-cell differentiation from nonendocrine epithelial cells of the adult human pancreas. Nat Med 12:310–316

Available online at www.sciencedirect.com
SCIENCE DIRECT
ELSEVIER
Immunology Letters 106 (2006) 82–90
Immunology Letters
www.elsevier.com/locate/

Modulation of acute graft-versus-host disease and chimerism after adoptive transfer of *in vitro*-expanded invariant Vα14 natural killer T cells

Masaki Kuwatani [a,b], Yoshinori Ikarashi [a,*], Akira Iizuka [a,d], Chihiro Kawakami [a], Gary Quinn [c], Yuji Heike [a], Mitsuzi Yoshida [a], Masahiro Asaka [b], Yoichi Takaue [d], Hiro Wakasugi [a,*]

[a] *Pharmacology Division, National Cancer Center Research Institute, 5-1-1 Tsukiji, Chuo-ku, Tokyo 104-0045, Japan*
[b] *Department of Gastroenterology, Graduate School of Medicine, Hokkaido University, Sapporo 060-8638, Japan*
[c] *Section for Studies on Metastasis, National Cancer Center Research Institute, 5-1-1 Tsukiji, Chuo-ku, Tokyo 104-0045, Japan*
[d] *Hematopoietic Stem Cell Transplantation/Immunotherapy Unit, National Cancer Center Hospital, Tokyo, Japan*

Received 22 February 2006; received in revised form 1 May 2006; accepted 3 May 2006
Available online 23 May 2006

Abstract

Mouse natural killer T cells with an invariant Vα14-Jα18 TCR rearrangement (Vα14i NKT cells) are able to regulate immune responses through rapid and large amounts of Th1 and Th2 cytokine production. It has been reported that *in vivo* administration of the Vα14i NKT cell ligand, α-galactosylceramide (α-GalCer) significantly reduced morbidity and mortality of acute graft-versus-host disease (GVHD) in mice. In this study, we examined whether adoptive transfer of *in vitro*-expanded Vα14i NKT cells using α-GalCer and IL-2 could modulate acute GVHD in the transplantation of spleen cells of C57BL/6 mice into (B6 × DBA/2) F_1 mice.

We found that the adoptive transfer of cultured spleen cells with a combination of α-GalCer and IL-2, which contained many Vα14i NKT cells, modulated acute GVHD by exhibiting long-term mixed chimerism and reducing liver damage. Subsequently, the transfer of Vα14i NKT cells purified from spleen cells cultured with α-GalCer and IL-2 also inhibited acute GVHD. This inhibition of acute GVHD by Vα14i NKT cells was blocked by anti-IL-4 but not by anti-IFN-γ monoclonal antibody. Therefore, the inhibition was dependent on IL-4 production by Vα14i NKT cells. Our findings highlight the therapeutic potential of *in vitro*-expanded Vα14i NKT cells for the prevention of acute GVHD after allogeneic hematopoietic stem cell transplantation.

Keywords: Graft-versus-host disease; NKT cell; α-Galactosylceramide; Chimerism

1. Introduction

Mouse natural killer T cells with an invariant Vα14-Jα18 TCR rearrangement (Vα14i NKT cells) are a unique T cell population that is specifically activated by a synthetic glycolipid, α-galactosylceramide (α-GalCer) in a non-classical MHC class I molecule CD1d-restricted manner [1]. Vα14i NKT cells are known as immunomodulating cells influencing the Th1/Th2 balance, mainly via rapid secretion of robust amounts of Th1 (such as IFN-γ) and Th2 (IL-4, IL-10 and IL-13) cytokines. Thus, Vα14i NKT cells have a critical role for various immune responses including autoimmune disease [2], tumor-immunity [3,4], infection and allogeneic transplantation [5].

Graft-versus-host disease (GVHD) is an intractable and severe obstacle in allogeneic hematopoietic stem cell transplantation (HSCT). To resolve this, various treatments such as donor T cell depletion [6] and immunosuppressive drugs [7] have been attempted. In mouse acute GVHD models, a Th1 dominant cytokine secretion profile and expansion of donor $CD8^+$ T cells have been reported [8–10]. Hence it is suggested that acute GVHD is reduced by the skewed Th2 polarization of host immunity and the suppression of donor $CD8^+$ T cell

Abbreviations: GVHD, graft-versus-host disease; HSCT, hematopoietic stem cell transplantation; α-GalCer, α-galactosylceramide; Vα14i NKT cells, natural killer T cells with an invariant Vα14-Jα18 TCR rearrangement; B6, C57BL/6; BDF_1, (B6 × DBA/2) F_1; SC, spleen cells; α-GCSC, SC were cultured with IL-2 and α-GalCer; mAb, monoclonal antibody; Vα24i NKT cells, NKT cells with an invariant Vα24-JαQ TCR rearrangement; GOT, glutamic oxaloacetic transaminase; GPT, glutamic pyruvic transaminase.

* Corresponding authors. Tel.: +81 3 3547 5248; fax: +81 3 3542 1886.
E-mail addresses: yikarash@gan2.ncc.go.jp (Y. Ikarashi), hwakasug@gan2.ncc.go.jp (H. Wakasugi).

0165-2478/$ – see front matter © 2006 Elsevier B.V. All rights reserved.
doi:10.1016/j.imlet.2006.05.001

expansion. It has been reported that immune-regulatory cells such as $CD4^+$ $CD25^+$ T cell [11], $NK1.1^+$ or $DX5^+$ T cells [5,12] reduced acute GVHD. Recently, it has been demonstrated that the administration of α-GalCer to induce IL-4 production by host Vα14i NKT cells suppressed acute GVHD in a mouse model [13,14], which suggests the potential of α-GalCer/NKT cell-based immunotherapy for the prevention of acute GVHD. Nevertheless, the frequency of human NKT cells with an invariant Vα24-JαQ TCR rearrangement paired with Vβ11 TCR (Vα24i NKT cells) is very low (less than 0.5%) in peripheral blood mononuclear cells [15]. Furthermore, it has been reported that the number of NKT cells in recipients of HSCT with acute GVHD is lower compared to those without acute GVHD [16]. Given that *in vivo* administration of α-GalCer could not expand host NKT cells in some cases [17,18], we hypothesized that an adoptive transfer of *in vitro*-expanded NKT cells would be more effective than *in vivo* administration of α-GalCer alone in patients with acute GVHD.

Several investigators have reported that human Vα24i NKT cells were effectively expanded using α-GalCer plus a combination of cytokines, such as IL-2, IL-7 and IL-15 *in vitro* [19–22], while mouse Vα14i NKT cells could also be expanded with α-GalCer *in vitro* [1,23]. We found that the culture of spleen cells with α-GalCer and IL-2 for 4 days efficiently induced the expansion of Vα14i NKT cells [24]. Moreover, we revealed that *in vitro*-expanded Vα14i NKT cells retained the ability to produce IL-4 and IFN-γ and migrated into peripheral organs after adoptive transfer [24]. Therefore, adoptive transfer of *in vitro*-expanded Vα14i NKT cells may reduce acute GVHD.

In this study, we demonstrated that adoptive transfer of *in vitro*-expanded Vα14i NKT cells reduced acute GVHD such as liver injury and maintained long-term mixed chimerism. This effect is dependent on IL-4 using neutralizing anti-IL-4 monoclonal antibody. Our findings indicate the therapeutic potential of *in vitro*-expanded Vα14i NKT cells for the prevention of acute GVHD.

2. Materials and methods

2.1. Mice

Female C57BL/6N (B6, H-2^b), DBA/2N (DBA/2, H-2^d) and (C57BL/6 × DBA/2) F_1 (BDF_1, H-$2^{b/d}$) mice were purchased from Charles River Japan (Kanagawa, Japan). All mice maintained in our animal facilities were 8–12 weeks of age at the time of transplantation. All animal protocols for this study were reviewed and approved by the committee for ethics of animal experimentation in the National Cancer Center.

2.2. Monoclonal antibodies and reagents

Fluorescein isothiocyanate (FITC)-conjugated mAb against H-$2K^d$ and phycoerythrin (PE)-conjugated mAb against CD3, CD4, CD8, B220, DX-5, NK1.1 were all purchased from BD Pharmingen (San Diego, CA). For blocking IL-4 and IFN-γ *in vivo*, anti-IL-4 (clone: 11B11) and anti-IFN-γ (clone: R4-6A2) mAb were obtained from the ascites of nude mice inoculated with the hybridomas. α-GalCer was kindly provided by Pharmaceutical Research Laboratory, KIRIN Brewery Co. Ltd. (Gunma, Japan). Recombinant human IL-2 was kindly donated by Takeda Chemical Ind. Ltd. (Osaka, Japan). PE or APC-conjugated CD1d/α-GalCer tetramer was prepared in a baculovirus expression system as previously described [25]. Mouse CD1d/β2-microglobulin expression vector was provided by Dr. M. Kronenberg (La Jolla Institute for Allergy and Immunology, San Diego, CA).

2.3. Cell culture and purification of Vα14i NKT cells

In vitro expansion of Vα14i NKT cells was performed as previously described [24]. Briefly, spleen cell (SC) suspensions (5×10^5 cells/ml) were cultured with α-GalCer (50 ng/ml) and recombinant human IL-2 (100 IU/ml) in RPMI 1640 culture medium (Sigma–Aldrich, Saint Louis, MO) supplemented with 8% fetal calf serum (JRH Biosciences, Lenexa, KS), penicillin (50 U/ml), streptomycin (50 μg/ml) and 2-mercaptoethanol (5×10^{-5} M) for 4 days in a 37 °C, 5% CO_2 incubator. In some experiments, *in vitro*-expanded Vα14i NKT cells were positively selected with PE-conjugated CD1d/α-GalCer tetramer, anti-PE microbeads and SuperMACS system (Miltenyi Biotec, Bergisch Gladbach, Germany), as preciously described [24]. In brief, dead cells were removed from cultured SC as described above using a dead cell removal kit (Miltenyi Biotec), LS column (Miltenyi Biotec) and SuperMACS system (Miltenyi Biotec). Then, the SC were preincubated with anti-CD16/32 (2.4G2, BD PharMingen), stained with appropriate diluted PE-conjugated CD1d/α-GalCer tetramer on ice in the dark for 30 min, and washed three times by buffer (phosphate buffered saline supplemented with 0.5% bovine serum albumin and 2 mM EDTA). The stained cells were then incubated with anti-PE microbeads (Miltenyi Biotec) (1×10^7 cells/microbeads in 40 μl) on ice in the dark for 30 min, suspended in 2 ml buffer, and finally passed through a LS column using the SuperMACS system with additive 3× 3 ml of buffer for washing column. Consequently, we acquired the purified Vα14i NKT cells as residual cells in the column. The purity of CD1d/α-GalCer $tetramer^+$ $CD3^+$ cells was more than 96%.

2.4. Cell transfer and treatment with antibodies

For the induction of GVHD, 7×10^7 spleen cells from B6 mice were transferred into BDF_1 mice intravenously through the tail vein (GVHD mice) as previously described [8]. One day later, 2×10^7 spleen cells cultured with α-GalCer and IL-2 for 4 days (α-GCSC) were injected intravenously into BDF_1 mice with GVHD. In other experiments, purified Vα14i NKT cells were transferred into GVHD mice. In some experiments, GVHD mice were administered with anti-IL-4 mAb (3 mg/mouse) or anti-IFN-γ mAb (1 mg/mouse) intraperitoneally on the day of α-GCSC transfer, referring previous reports for effective doses of mAbs [26–28].

2.5. Flow cytometry

The phenotype of cells was determined by multicolor flow cytometory as previously described [24]. To prevent non-specific binding of mAb, cells were pre-incubated with anti-CD16/32 (2.4G2, BD PharMingen). The relative percentages of host- and donor-origin cells in the recipient spleens were determined by anti-H2-K^d (recipient type) as an indicator of GVHD in which donor chimerism was elevated [29]. The relative percentage of donor-origin cells (% donor chimerism) in chimeric recipients was calculated by the following formula: 100 − %H-2K^d positive cells.

In addition, for the determination of a lineage-specific chimerism, recipient spleens were stained with FITC-conjugated antibody against H-2K^d and PE-conjugated antibodies against CD3, CD4, CD8, B220, DX-5. Vα14i NKT cell frequency was determined by FITC-conjugated CD3 and APC-conjugated CD1d/α-GalCer tetramer. Propidium iodide was used to exclude dead cells. The stained cells were analyzed using FACSCalibur (BD Biosciences, San Jose, CA) and Flow Jo software (Tree Star Inc., San Carlos, CA).

2.6. Assessment of GVHD

Recipient mice were sacrificed on day 14. The serum glutamic oxaloacetic transaminase (GOT) and glutamic pyruvic transaminase (GPT) levels were detected (SRL Inc., Tokyo, Japan) by serological examination using standard methodologies. Additionally, liver and small bowel were embedded in paraffin, cut into 5 μm-thick sections, and stained with H&E for histological examination.

3. Results

3.1. Adoptive transfer of spleen cells cultured with α-GalCer and IL-2 (α-GCSC) inhibit donor T cell engraftment in mice with acute GVHD.

In order to obtain a large number of Vα14i NKT cells, spleen cells from BDF_1 mice were cultured with α-GalCer and IL-2 for 4 days as previously reported [24]. As shown in Fig. 1A, the percentage of $CD3^+$ CD1d/α-GalCer $tetramer^+$ cells increased approximately 20-fold after expansion in culture. In

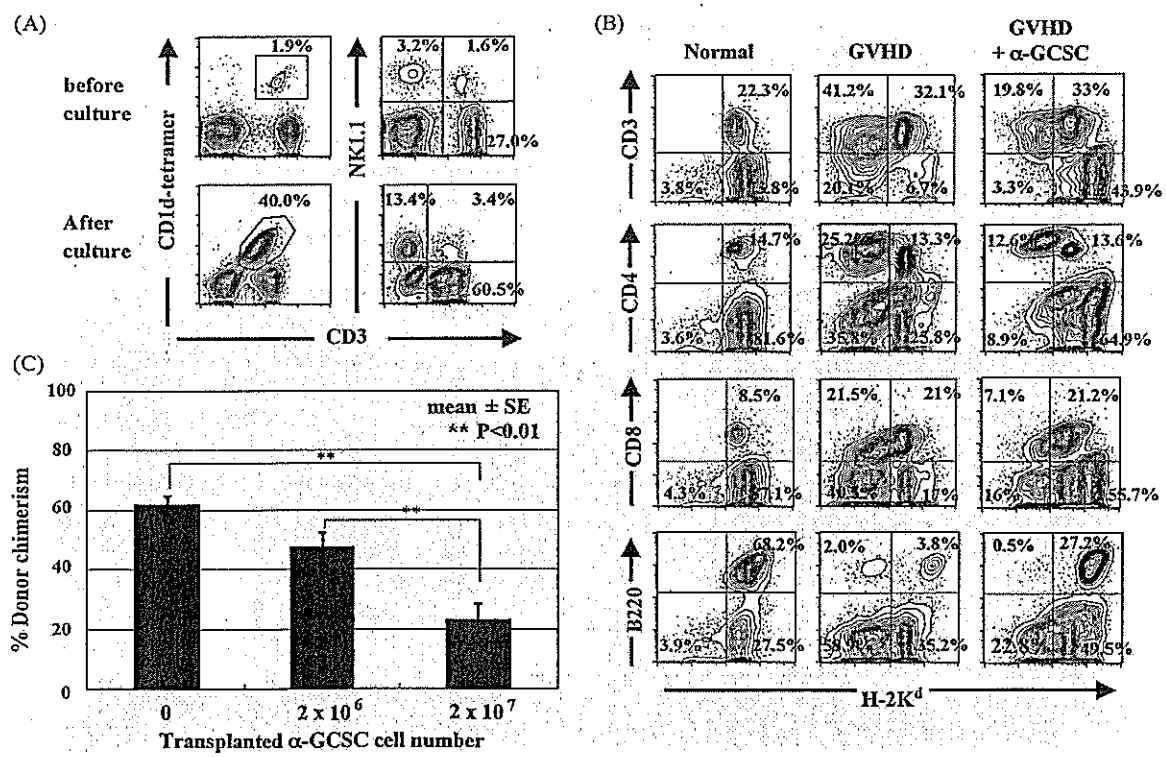

Fig. 1. Adoptive transfer of spleen cells cultured with α-GalCer and IL-2 reduced percentages of donor chimerism depending on cell number. (A) Spleen cells (SC) of BDF_1 mice were cultured with 50 ng/ml α-GalCer and 100 IU/ml IL-2 for 4 days. The percentage of Vα14i NKT cells and $NK1.1^+$ $CD3^-$ NK cells were determined. Before and after culture cells were stained with anti-CD3-FITC, anti-NK1.1-PE mAb and CD1d/α-GalCer tetramer-APC. The numbers in each of the quadrants represent the percentage of total analyzed cells. The fluorescence profiles are representative of at least three independent experiments. (B, C) BDF_1 mice were transferred with 7×10^7 B6 SC on day 0 for GVHD induction and with or without α-GCSC as indicated at 2×10^7 or 2×10^6 on day 1 and then donor chimerism and surface phenotype of SC were analyzed by flow cytometory on day 14. (B) SC of untreated (normal: left column), transplanted with B6 SC alone (GVHD: center column) and transplanted with both B6 SC and 2×10^7 α-GCSC (GVHD + α-GCSC: right column) mice were stained with anti-H-2K^d-FITC and each of anti-CD3, CD4, CD8, B220, DX-5-PE mAb at day 14. The numbers in each of the quadrants represent the percentage of total analyzed cells. The fluorescence profiles are representative of at least three independent experiments. (C) The bars indicate averages of percentage of donor chimerism with standard error of the mean. The number of each group is α-GCSC transfer of 0: $n=6$; 2×10^6: $n=6$; 2×10^7: $n=7$. $^{**}p<0.01$ versus group of α-GCSC transfer of 0. The differences between groups were analyzed using non-repeated measures ANOVA with Bonferroni correction. Data are representative of three independent experiments.

addition, $CD3^-$ $NK1.1^+$ cells (NK cells) in α-GCSC were also expanded 2.5-fold. To investigate whether α-GCSC containing large amounts of Vα14i NKT cells could inhibit acute GVHD, we transplanted BDF_1 mice with 7×10^7 spleen cells from B6 on day 0 for GVHD induction and α-GCSC (2×10^7 or 2×10^6 cells) on day 1. Normal mice received saline only on day 1. At day 14, mice transplanted with spleen cells from B6 mice alone (GVHD mice) exhibited donor-dominant chimerism (% donor chimerism (mean ± S.E.M.): 61.7 ± 3.0%) and expansion of donor $CD3^+$ cells (41%) including both $CD4^+$cells (25.2%) and $CD8^+$ cells (21.5%), while mice transplanted with B6 SC plus 2×10^7 α-GCSC had reduced donor chimerism (% donor chimerism (mean ± S.E.M.): 22.9 ± 5.6), lower engraftment of donor $CD4^+$ cells (12.6%) and $CD8^+$ cells (7.1%) as compared with GVHD mice (Fig. 1B and 1C). These data indicate that the transfer of α-GCSC suppressed early donor T cell engraftment. However, lower number of α-GCSC (2×10^6 cells) did not significantly inhibit donor cell engraftment (Fig. 1C).

3.2. Adoptive transfer of α-GCSC reduces symptoms of acute GVHD

Next, we examined whether the transfer of α-GCSC ameliorate serological and histological findings of acute GVHD, by analyzing the serum levels of GOT and GPT, and histology of liver tissue specimens. The serum GOT levels of GVHD mice

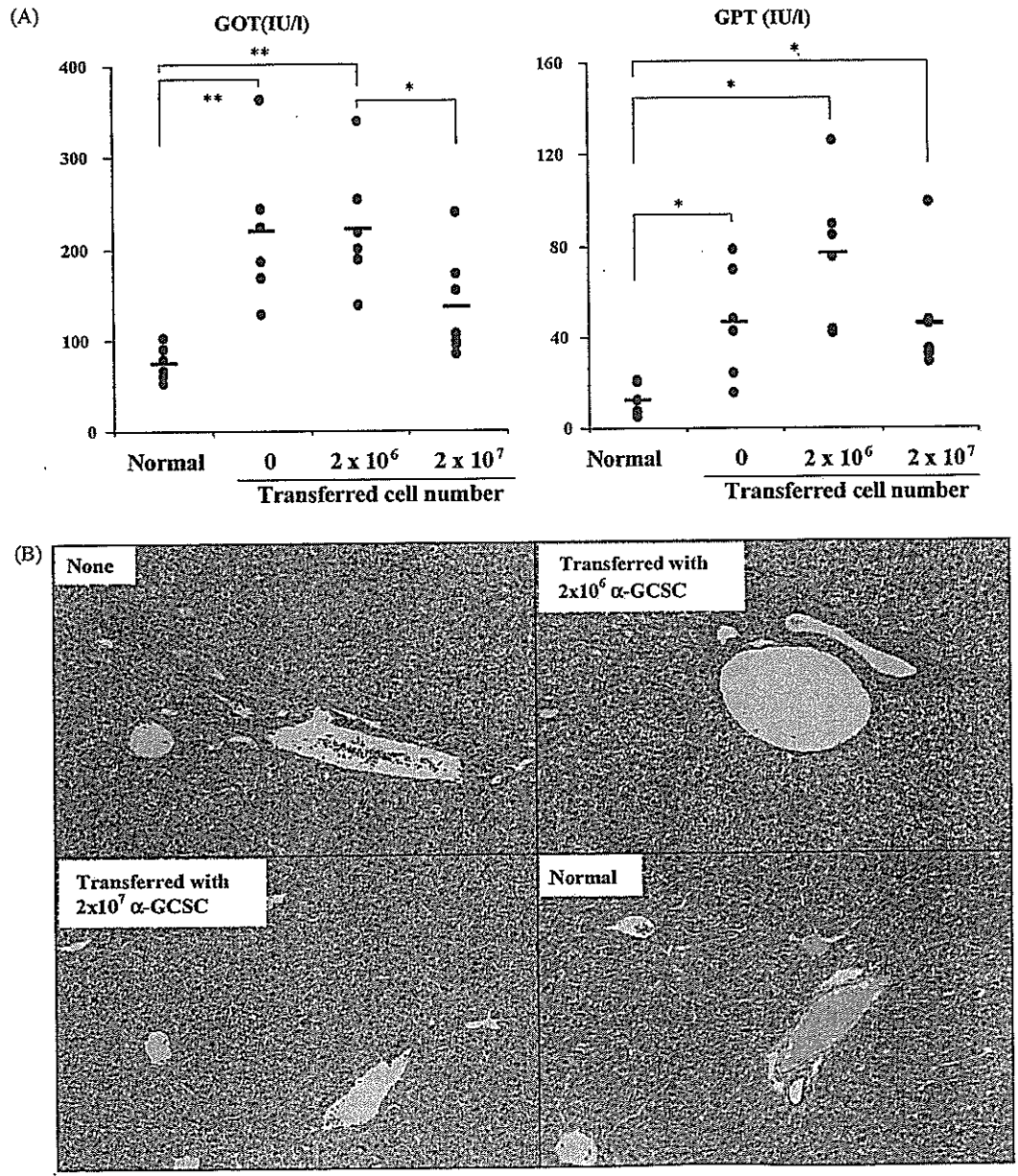

Fig. 2. Transplanted BDF_1 α-GCSC alleviated GVHD signs serologically and histologically. (A) Induction of GVHD and infusion of α-GCSC were performed as described in Fig. 1. The serum GOT levels of mice group with 2×10^7 α-GCSC were low compared with other GVHD mice groups ($^*p < 0.05$ and $^{**}p < 0.01$ by non-repeated measures ANOVA and Bonferroni correction), although the serum GPT levels of all mice groups were significantly high compared with normal ($n = 6$). (B) Histology of liver tissue of GVHD mice with or without α-GCSC as described above and normal. Representative of three independent experiments of each group is shown.

were significantly higher as compared with untreated control mice, whereas the serum GOT levels in GVHD mice transferred with 2×10^7 α-GCSC were reduced by 50% as compared with GVHD mice (Fig. 2A). The reduction of serum GOT was not observed when transferred with 2×10^6 α-GCSC. Serum GPT levels were not significantly different among all groups (Fig. 2A). Histological analysis showed remarkable hepatic lymphocyte infiltration in the portal area in GVHD mice, while very little or no infiltration was detected in GVHD mice transferred with 2×10^7 α-GCSC. Mice treated with 2×10^6 α-GCSC showed no reduction in lymphocyte infiltration (Fig. 2B). These results indicate that α-GCSC alleviated acute GVHD and retarded donor T cell engraftment. However, spleen cells containing about 3% Vα14i NKT cells cultured with IL-2 alone could not inhibit acute GVHD and rapid donor T cell engraftment (data not shown), suggesting that the inhibitory effect of α-GCSC on GVHD is mainly attributable to the potential of Vα14i NKT cells.

3.3. Maintenance of donor cell engraftment and mixed chimerism in GVHD mice requires IL-4 but not IFN-γ following adoptive transfer of α-GCSC

Next, we examined whether the inhibition of acute GVHD was due to rapid rejection and/or graft failure by α-GCSC. Long-term donor chimerism was observed in GVHD mice with or without α-GCSC (2×10^7 cells) at 14, 42 and 100 days after the induction of GVHD (Fig. 3A). GVHD mice exhibited complete donor chimerism at day 100. Approximately 20% donor chimerism was observed in GVHD mice when treated with α-GCSC at day 14, and this gradually increased to 35% by day 100. Therefore, GVHD mice with α-GCSC sustained mixed chimerism for a significant period of time. Donor-derived lymphocytes in these mice contained T cells ($CD4^+$ and $CD8^+$) and B cells (Fig. 3B). Although very few donor-derived B cells (0.5%) were detected at 14 days after induction of GVHD with α-GCSC administration, 6% donor-derived B cells were appeared in GVHD mice with α-GCSC at 100 days. These results suggest that the transfer of α-GCSC did not impair donor cell engraftment or maintenance of long-term mixed chimerism.

It has been known that activated Vα14i NKT cells rapidly produced IL-4 and IFN-γ [23,24]. We therefore examined whether IL-4 and/or IFN-γ produced by Vα14i NKT cells is the cytokine(s) responsible for mediating inhibition of GVHD. Neutralizing mAbs against IL-4 and IFN-γ were administered intraperitoneally into GVHD mice with or without α-GCSC. As shown in Fig. 4, administration of anti-IL-4 or anti-IFN-γ mAb had no effect on donor chimerism of GVHD mice. However, the inhibitory effect on GVHD by a transfer of α-GCSC

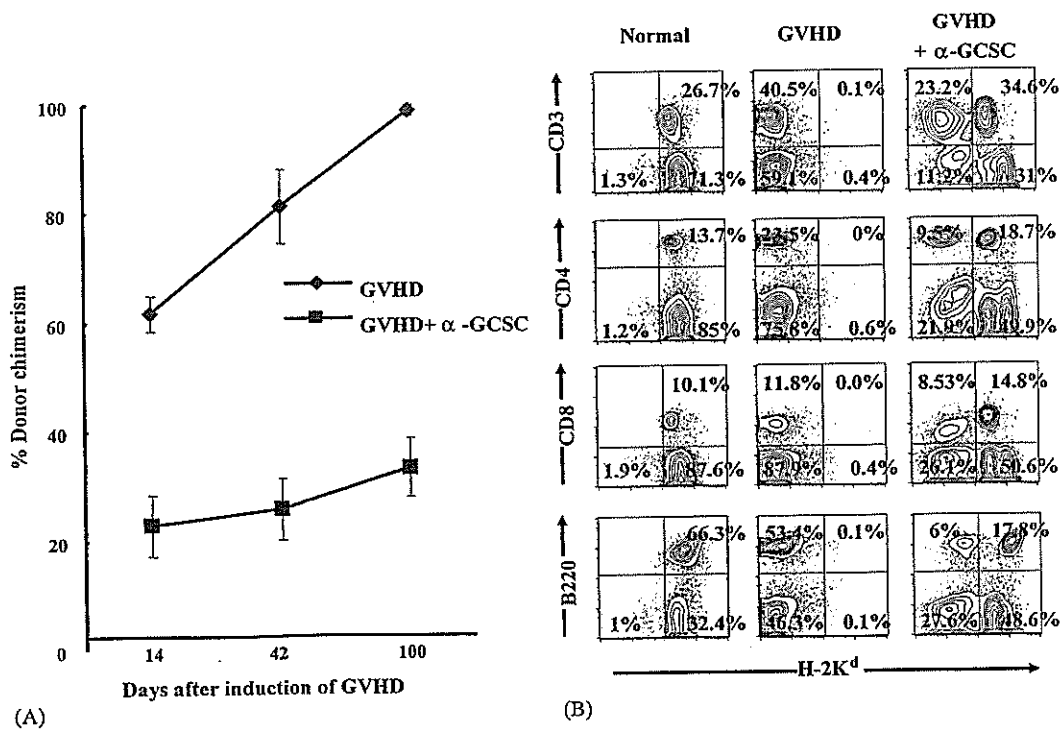

Fig. 3. Donor cells were not rejected and mixed chimerism was maintained in GVHD mice with α-GCSC for a long term. (A) Induction of GVHD and a transfer of α-GCSC were performed as described in Fig. 1. SC of GVHD mice transplanted with or without α-GCSC were stained with anti-H-$2K^b$ mAb and then donor chimerism was determined on days 14, 42 and 100 after GVHD induction. Percentages of donor chimerism in SC of GVHD mice transplanted with α-GCSC gradually increased as days passed. GVHD indicates GVHD mice without transfer of α-GCSC ($n=6$ on day 14, $n=6$ on day 42, $n=4$ on day 100); GVHD + cultured SC, GVHD mice with transfer of α-GCSC ($n=7$ on day 14, $n=5$ on day 42, $n=4$ on day 100). Values are mean ± S.E.M. on days 14, 42 and 100. $^{**}p<0.01$ versus group of GVHD. (B) SC of untreated (normal: the left column), transplanted with B6 SC alone (GVHD: the center) and transplanted with both B6 SC and 2×10^7 α-GCSC (GVHD + cultured SC: the right) mice were stained with anti-H-$2K^d$-FITC and each of anti-CD3, CD4, CD8, B220, DX-5-PE mAb on day 100. The numbers in each of the quadrants represent the percentage of total analyzed cells. The fluorescence profiles are representative of at least three independent experiments.

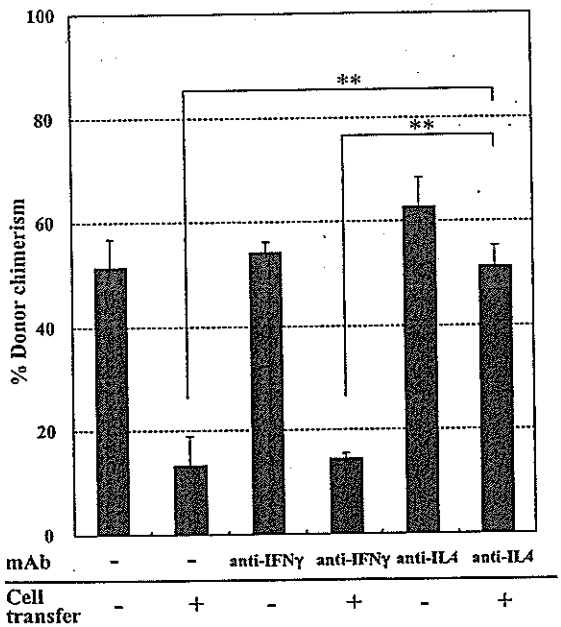

Fig. 4. GVHD was inhibited by the function of BDF_1 α-GCSC depending on IL-4, but not IFN-γ. Induction of GVHD and a transfer of α-GCSC were performed as described in Fig. 1. GVHD mice with or without α-GCSC were injected with or without anti-IL-4 (3 mg/mouse) or IFN-γ (1 mg/mouse) neutralizing mAbs on day 1. Donor chimerism was determined by anti-H-$2K^b$ mAb on day 14. Values are mean ± SEM on day 14. The number of each group is from the left $n = 5, 6, 6, 4, 4$ and 5, respectively.

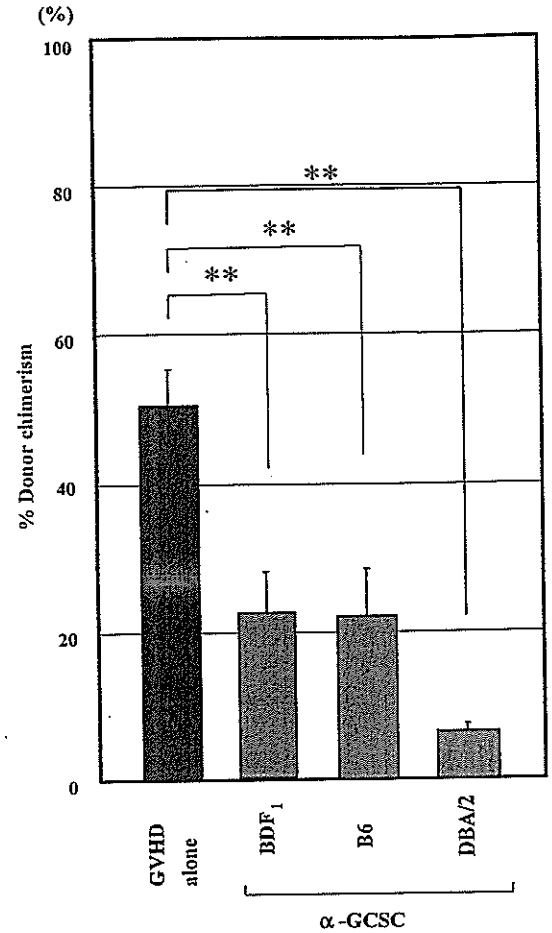

Fig. 5. α-GCSC from B6 or DBA/2 mice could also inhibit GVHD. Induction of GVHD and infusion of α-GCSC were performed as described in Fig. 1. The percentages of donor cell chimerism at day 14 in GVHD mice with any α-GCSC was significantly lower compared with GVHD mice with none (GVHD). The number of each group is GVHD (GVHD mice with none), $n = 15$; BDF_1, $n = 7$; B6, $n = 6$; DBA/2, $n = 6$. $^{**}p < 0.01$ versus group of GVHD by non-repeated measures ANOVA and Bonferroni correction.

was blocked by anti-IL-4, but not by anti-IFN-γ mAb (Fig. 4). Therefore, the retardation of donor cell engraftment and alleviation of acute GVHD by α-GCSC appears to be mediated by an IL-4-dependent mechanism.

3.4. *Purified in vitro-expanded Vα14i NKT cells ameliorated acute GVHD*

We next determined whether α-GCSC derived from the parental strain (B6 or DBA/2) could also inhibit rapid donor cell engraftment. Firstly, α-GCSC containing 30 or 15% of Vα14i NKT cells in B6 mice or DBA/2 mice, respectively, were transferred (2×10^7) into GVHD mice. Expectedly, transfer of α-GCSC, originating from both B6 and DBA/2 mice reduced the percentage of donor chimerism in GVHD mice (Fig. 5). The results suggest that the inhibitory effect of α-GCSC on GVHD was not related to their strain of origin.

To examine which cell compartment in the α-GCSC inhibits acute GVHD, Vα14i NKT cells were purified from α-GCSC by using CD1d/α-GalCer tetramer and MACS system. The purity of Vα14i NKT cells was more than 96% (Fig. 6A). Donor chimerism of GVHD mice injected with 4×10^6 purified Vα14i NKT cells (nearly equivalent to 2×10^7 α-GCSC) was lower than that of mice with GVHD alone, although it was higher than that of GVHD mice transplanted with 2×10^7 of α-GCSC (Fig. 6B). This data indicates that transfer of purified Vα14i NKT cells alone can ameliorate GVHD.

4. Discussion

Vα14i NKT cells play an important role in immune regulation including autoimmunity, tumor immunity and infection. Furthermore, it has been demonstrated that $NK1.1^+$ NKT cells from donor bone marrow [5] or residual host [30] can inhibit acute GVHD. Recently, several groups reported that *in vivo* administration of the Vα14i NKT cell specific ligand, α-GalCer, modulated acute GVHD and prolonged survival [13,14,31]. These studies suggest the therapeutic potential of α-GalCer or Vα14i NKT cells for the prevention of acute GVHD after allogeneic HSCT.

Although we also obtained similar results regarding the inhibition of GVHD by α-GalCer-activated Vα14i NKT cells, we used *in vitro*-expanded Vα14i NKT cells and non-myeloablative F_1 mice as recipients. It is likely that this difference led to the distinct results in regard to the difference in donor chimerism. We found that GVHD mice with a transfer of Vα14i NKT cells could maintain mixed chimerism (donor chimerism frequency of 20–30%) for a long period. By contrast, Morecki et al. trans-

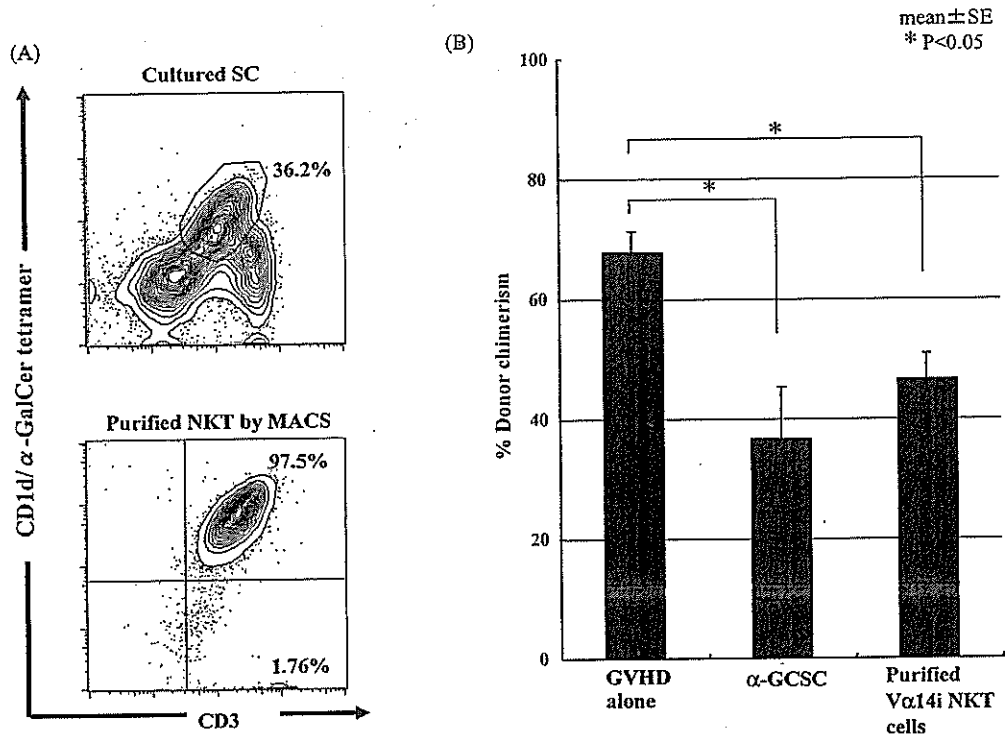

Fig. 6. Purified Vα14i NKT cells from BDF_1 α-GCSC also alleviated GVHD. (A, B) Induction of GVHD and cell culture were performed as described in Fig. 1. The purification of NKT cells from BDF_1 α-GCSC was done as described in materials and methods. (A) Before and after the purification of NKT cells, BDF_1 α-GCSC were stained with anti-CD3-FITC and CD1d/α-GalCer tetramer-APC or CD1d/α-GalCer tetramer-PE mAb. The numbers in each of the quadrants represent the percentage of total analyzed cells. The fluorescence profiles are representative of at least three independent experiments. (B) Mice were additionally infused with or without 2×10^7 BDF_1 α-GCSC or 4×10^6 purified NKT cells from α-GCSC by MACS system. The percentage of donor cell chimerism in SC in each mouse was determined on day 14. The number of each group is GVHD (GVHD mice with none), $n=6$; α-GCSC 2×10^7, $n=5$; isolated Vα14i NKT cells 4×10^6, $n=6$. $^{**}p<0.01$ versus group of GVHD by non-repeated measures ANOVA and Bonferroni correction.

planted spleen cells of parental B6 mice into low dose total body irradiated (BALB/c × B6) F_1 mice similar to our GVHD model and showed that the donor chimerism of α-GalCer- administered mice was very low (2% of donor chimerism). This difference in donor chimerism between a transfer of Vα14i NKT cells and an injection with α-GalCer seems to be attributable to IL-4, although previous studies [14,31] and our current results demonstrated that IL-4 from Vα14i NKT cells mainly contributed to the inhibition of acute GVHD. It has been reported that the amount and time course of serum IL-4 levels were distinct between direct administration of α-GalCer and the transfer of α-GalCer pulsed dendritic cells [32]. Direct administration of α-GalCer induced more rapid and higher levels of serum IL-4 levels as compared with α-GalCer-pulsed dendritic cells. We propose that the distinct donor chimerism in GVHD mice between a transfer of Vα14i NKT cells and an injection with α-GalCer may be attributable to the different amount and time course of serum IL-4 levels. Furthermore, we measured Th polarization (IL-4 and IFN-γ production) in total (donor plus recipient) cells 7 days after transplantation by ELISA assay and found a Th2 dominant response (data not shown). However, we do not know if a Th2 dominant response differed between donor and recipient derived cells.

Previous reports [29,33,34] indicated that rapid engraftment of donor cells was always accompanied by severe GVHD, and that, conversely, slow engraftment led to a reduction of GVHD. Pan et al. [35] also showed that a stable and lower level of donor chimerism should be enough to induce donor–recipient reciprocal tolerance. Thus, their and our data show that IL-4-dependent retention of mixed chimerism or a gradual transition from a mixed to a complete chimera by transfer of α-GCSC leads to alleviation of GVHD. It should be noted, however, that systemic administration of IL-4 is ineffective or toxic [36]. Moreover, a stable mixed chimerism of GVHD mice transplanted with Vα14i NKT cells was sustained for an expanded period. These results suggest that the stable chimerism induced by Vα14i NKT cells is not due to graft rejection.

α-GCSC including $CD1d^+$ cells loaded with α-GalCer activated recipient Vα14i NKT cells (data not shown). Therefore, both recipient and transferred Vα14i NKT cells might contribute to alleviation of GVHD as previously reported [31]. However, we showed that inhibition of GVHD by Vα14i NKT cells was due to IL-4 produced exclusively by Vα14i NKT cells among α-GCSC [24], and that a transfer of purified Vα14i NKT cells alone prevented acute GVHD. These data suggest that transferred Vα14i NKT cells were sufficient to modulate acute GVHD.

Recently, Haraguchi et al. [31] reported the effect of *in vivo* administration of α-GalCer and the adoptive transfer of NKT cells on the prevention of GVHD. This seems to be logical considering the relationship between host-residual and transferred NKT cells as they mentioned that host-residual, but not

transferred, NKT cells are essential for amelioration of GVHD. Although the authors indicated that maximal GVHD reduction and survival were mainly accompanied by graft rejection, our data demonstrated that effective GVHD reduction was accompanied by maintenance of mixed chimerism. This discrepancy may be explained by the different GVHD settings, non-myeloablative and myeloablative recipients, and by the balance between the dose of alloreactive donor cells and the activity of host-residual NKT cells.

Although several studies have reported that the number of circulating NKT cells was reduced in cancer patients [17,37,38], direct injection of α-GalCer is not expected to induce anti-tumor effects. On the other hand, adoptive *in vitro*-expanded NKT cell immunotherapy may be useful for cancer therapy. In support of this, we found that adoptive transfer of *in vitro*-expanded Vα14i NKT cells could prevent lung tumor metastasis in a mouse model (unpublished data Ikarashi et al.). We believe that adoptive transfer of NKT cell therapy combined with allogenic HSCT may be beneficial for cancer patients, because of NKT cell function for prevention of GVHD and anti-tumor effects.

Acknowledgments

We thank Pharmaceutical Research Laboratory, Kirin Brewery Co. (Gumma, Japan) for providing α-GalCer and thank Dr. Kazuyoshi Takeda (Juntendo University, Tokyo, Japan) for providing hybridoma cell lines. This work was supported in part by a grant-in-aid for the Third-Term Comprehensive 10-Year Strategy for Cancer Control from the Ministry of Health, Labour and Welfare, Japan and Research Resident Fellowship from the Foundation for Promotion of Cancer Research, Japan (M. Kuwatani).

References

[1] Kawano T, Cui J, Koezuka Y, Toura I, Kaneko Y, Motoki K, et al. CD1d-restricted and TCR-mediated activation of Vα14 NKT cells by glycosylceramides. Science 1997;278:1626–9.

[2] Hammond KJ, Poulton LD, Palmisano LJ, Silveira PA, Godfrey DI, Baxter AG. α/β-T cell receptor (TCR)$^+$CD4$^-$CD8$^-$ (NKT) thymocytes prevent insulin-dependent diabetes mellitus in non-obese diabetic (NOD)/Lt mice by the influence of interleukin (IL)-4 and/or IL-10. J Exp Med 1998;187:1047–56.

[3] Moodycliffe AM, Nghiem D, Clydesdale G, Ullrich SE. Immune suppression and skin cancer development: regulation by NKT cells. Nat Immunol 2000;1:521–5.

[4] Kikuchi A, Nieda M, Schmidt C, Koezuka Y, Ishihara S, Ishikawa Y, et al. *In vitro* anti-tumor activity of α-galactosylceramide-stimulated human invariant Vα24$^+$ NKT cells against melanoma. Br J Cancer 2001;85:741–6.

[5] Zeng D, Lewis D, Dejbakhsh-Jones S, Lan F, Garcia-Ojeda M, Sibley R, et al. Bone marrow NK1.1$^-$ and NK1.1$^+$ T cells reciprocally regulate acute graft-versus-host disease. J Exp Med 1999;189:1073–81.

[6] Burnett AK, Hann IM, Robertson AG, Alcorn M, Gibson B, McVicar I, et al. Prevention of graft-versus-host disease by *in vitro* T cell depletion: reduction in graft failure with augmented total body irradiation. Leukemia 1988;2:300–3.

[7] Deeg HJ. Prophylaxis and treatment of acute graft-versus-host disease: current state, implications of new immunopharmacologic compounds and future strategies to prevent and treat acute GVHD in high-risk patients. Bone Marrow Transplant 1994;14(Suppl 4):S56–60.

[8] Via CS, Sharrow SO, Shearer GM. Role of cytotoxic T lymphocytes in the prevention of lupus-like disease occurring in a murine model of graft-versus-host disease. J Immunol 1987;139:1840–9.

[9] Rus V, Svetic A, Nguyen P, Gause WC, Via CS. Kinetics of Th1 and Th2 cytokine production during the early course of acute and chronic murine graft-versus-host disease. Regulatory role of donor CD8$^+$ T cells. J Immunol 1995;155:2396–406.

[10] Allen RD, Staley TA, Sidman CL. Differential cytokine expression in acute and chronic murine graft-versus-host-disease. Eur J Immunol 1993;23:333–7.

[11] Edinger M, Hoffmann P, Ermann J, Drago K, Fathman CG, Strober S, et al. CD4$^+$CD25$^+$ regulatory T cells preserve graft-versus-tumor activity while inhibiting graft-versus-host disease after bone marrow transplantation. Nat Med 2003;9:1144–50.

[12] Baker J, Verneris MR, Ito M, Shizuru JA, Negrin RS. Expansion of cytolytic CD8$^+$ natural killer T cells with limited capacity for graft-versus-host disease induction due to interferon γ production. Blood 2001;97:2923–31.

[13] Morecki S, Panigrahi S, Pizov G, Yacovlev E, Gelfand Y, Eizik O, et al. Effect of KRN7000 on induced graft-vs-host disease. Exp Hematol 2004;32:630–7.

[14] Hashimoto D, Asakura S, Miyake S, Yamamura T, Van Kaer L, Liu C, et al. Stimulation of host NKT cells by synthetic glycolipid regulates acute graft-versus-host disease by inducing Th2 polarization of donor T cells. J Immunol 2005;174:551–6.

[15] Godfrey DI, Hammond KJ, Poulton LD, Smyth MJ, Baxter AG. NKT cells: facts, functions and fallacies. Immunol Today 2000;21:573–83.

[16] Haraguchi K, Takahashi T, Hiruma K, et al. Recovery of Vα24$^+$ NKT cells after hematopoietic stem cell transplantation. Bone Marrow Transplant 2004;34:595–602.

[17] Giaccone G, Punt CJ, Ando Y, Ruijter R, Nishi N, Peters M, et al. A phase I study of the natural killer T-cell ligand α-galactosylceramide (KRN7000) in patients with solid tumors. Clin Cancer Res 2002;8:3702–9.

[18] Nieda M, Okai M, Tazbirkova A, Lin H, Yamaura A, Ide K, et al. Therapeutic activation of Vα24$^+$Vβ11$^+$ NKT cells in human subjects results in highly coordinated secondary activation of acquired and innate immunity. Blood 2004;103:383–9.

[19] Lin H, Nieda M, Nicol AJ. Differential proliferative response of NKT cell subpopulations to *in vitro* stimulation in presence of different cytokines. Eur J Immunol 2004;34:2664–71.

[20] Brossay L, Chioda M, Burdin N, Koezuka Y, Casorati G, Dellabona P, et al. CD1d-mediated recognition of an α-galactosylceramide by natural killer T cells is highly conserved through mammalian evolution. J Exp Med 1998;188:1521–8.

[21] Nishi N, van der Vliet HJ, Koezuka Y, von Blomberg BM, Scheper RJ, Pinedo HM, et al. Synergistic effect of KRN7000 with interleukin-15, -7, and -2 on the expansion of human Vα 24$^+$Vβ 11$^+$ T cells *in vitro*. Hum Immunol 2000;61:357–65.

[22] van der Vliet HJ, Nishi N, Koezuka Y, von Blomberg BM, van den Eertwegh AJ, Porcelli SA, et al. Potent expansion of human natural killer T cells using α-galactosylceramide (KRN7000)-loaded monocyte-derived dendritic cells, cultured in the presence of IL-7 and IL-15. J Immunol Meth 2001;247:61–72.

[23] Kronenberg M, Gapin L. The unconventional lifestyle of NKT cells. Nat Rev Immunol 2002;2:557–68.

[24] Ikarashi Y, Iizuka A, Heike Y, Yoshida M, Takaue Y, Wakasugi H. Cytokine production and migration of in-vitro expanded NK1.1$^-$ invariant Vα14 natural killer T (Vα14i NKT) cells using α-galactosylceramide and IL-2. Immunol Lett 2005;101:160–7.

[25] Matsuda JL, Naidenko OV, Gapin L, Nakayama T, Taniguchi M, Wang CR, et al. Tracking the response of natural killer T cells to a glycolipid antigen using CD1d tetramers. J Exp Med 2000;192:741–54.

[26] Yoshino S, Murata Y, Ohsawa M. Successful induction of adjuvant arthritis in mice by treatment with a monoclonal antibody against IL-4. J Immunol 1998;161:6904–8.

[27] Puliaev R, Nguyen P, Finkelman FD, Via CS. Differential requirement for IFN-γ in CTL maturation in acute murine graft-versus-host disease. J Immunol 2004;173:910–9.
[28] Carnaud C, Lee D, Donnars O, Park SH, Beavis A, Koezuka Y, et al. Cutting edge: cross-talk between cells of the innate immune system: NKT cells rapidly activate NK cells. J Immunol 1999;163:4647–50.
[29] Xun CQ, Tsuchida M, Thompson JS. Delaying transplantation after total body irradiation is a simple and effective way to reduce acute graft-versus-host disease mortality after major H2 incompatible transplantation. Transplantation 1997;64:297–302.
[30] Lan F, Zeng D, Higuchi M, Huie P, Higgins JP, Strober S. Predominance of NK1.1$^+$TCRαβ$^+$ or DX5$^+$TCRαβ$^+$ T cells in mice conditioned with fractionated lymphoid irradiation protects against graft-versus-host disease: "natural suppressor" cells. J Immunol 2001;167:2087–96.
[31] Haraguchi K, Takahashi T, Matsumoto A, Asai T, Kanda Y, Kurokawa M, et al. Host-residual invariant NK T cells attenuate graft-versus-host immunity. J Immunol 2005;175:1320–8.
[32] Fujii S, Shimizu K, Kronenberg M, Steinman RM. Prolonged IFN-γ-producing NKT response induced with α-galactosylceramide-loaded DCs. Nat Immunol 2002;3:867–74.
[33] Ritchie DS, Morton J, Szer J, Robert AW, Durrant S, Shuttleworth P, et al. Graft-versus-host disease, donor chimerism, and organ toxicity in stem cell transplantation after conditioning with fludarabine and melphalan. Biol Blood Marrow Transplant 2003;9:435–42.
[34] Childs R, Clave E, Contentin N, Jayasekera D, Hensel N, Leitman S, et al. Engraftment kinetics after non-myeloablative allogeneic peripheral blood stem cell transplantation: full donor T-cell chimerism precedes alloimmune responses. Blood 1999;94:3234–41.
[35] Pan Y, Luo B, Sozen H, Kalscheuer H, Blazar BR, Sutherland DE, et al. Blockade of the CD40/CD154 pathway enhances T-cell-depleted allogeneic bone marrow engraftment under non-myeloablative and irradiation-free conditioning therapy. Transplantation 2003;76:216–24.
[36] Atkinson K, Matias C, Guiffre A, Seymour R, Cooley M, Biggs J, et al. In vivo administration of granulocyte colony-stimulating factor (G-CSF), granulocyte-macrophage CSF, interleukin-1 (IL-1), and IL-4, alone and in combination, after allogeneic murine hematopoietic stem cell transplantation. Blood 1991;77:1376–82.
[37] Motohashi S, Kobayashi S, Ito T, Magara KK, Mikuni O, Kamada N, et al. Preserved IFN-α production of circulating Vα24 NKT cells in primary lung cancer patients. Int J Cancer 2002;102:159–65.
[38] Molling JW, Kolgen W, van der Vliet HJ, Boomsma MF, Kruizenga H, Smorenburg CH, et al. Peripheral blood IFN-γ-secreting Vα24$^+$Vβ11$^+$ NKT cell numbers are decreased in cancer patients independent of tumor type or tumor load. Int J Cancer 2005;116:87–93.